



Omission of intermediate stiffeners in box link beams using trapezoidal corrugated webs

Nader Fanaie^{a,*}, Danial Pesaran Behbahani^a, Samira Ebrahimi^b

^a Department of Civil Engineering, K. N. Toosi University of Technology, Tehran, Iran

^b School of Civil Engineering, College of Engineering, University of Tehran, Iran

ARTICLE INFO

Keywords:

Box link beam
Intermediate stiffeners
Corrugated web plates
Web shear buckling
Finite element modeling

ABSTRACT

In box link beams, intermediate stiffeners are often used to delay local shear bucklings, but welding operations in order to connect the intermediate stiffeners to the web of box link beams lead to increased construction costs, reduced execution speed, creating residual stresses and geometric imperfections, and weakening of materials at the junction of stiffeners to the web. The present study investigated corrugating webs of box link beams as an alternative to flat webs with intermediate stiffeners using Abaqus finite element software. First, equations were presented to determine the slenderness ratio and critical inelastic buckling stress of trapezoidal corrugated plates used as the web of box link beams. A comparison between box link beams with corrugated webs and box link beams with flat webs and intermediate stiffeners showed that box link beams with corrugated webs experienced more buckling stability, ductility, and energy dissipation due to the intrinsic geometrical characteristics of this type of web plate. The results of this study revealed that the use of trapezoidal corrugated webs in box link beams, if the geometric parameters of the corrugated webs are appropriately selected, can increase the maximum permissible compactness ratio of the web up to about 12% and 200% more compared to box link beams with flat webs and with or without intermediate stiffeners, respectively; Also, the energy dissipation of the box link specimens can be increased by about 20%.

1. Introduction

Eccentrically braced frames (EBFs) have a combination of the advantages of suitable ductility of moment-resisting frames and suitable lateral stiffness of concentrically braced frames. In eccentrically braced frames, braces are not allowed to buckle; consequently, the stable behavior of the system under severe earthquakes is guaranteed if the link beam behaves appropriately. In eccentrically braced frames, the link beam is introduced as a structural fuse and as a result, the behavior of the link beam determines the overall behavior of the eccentrically braced frame. In these systems, nonlinear behavior is limited only to the link beam, and other frame members must behave elastically. With respect to the yielding mechanism, the link beams are divided into three categories: short, intermediate, and long link beams. In short link beams, energy dissipation occurs through shear yielding of the web and as a result, these link beams are also called shear link beams. Comparison of short link beams with long link beams showed that the link beam's seismic responses such as elastic lateral stiffness, ductility, energy

dissipation and ultimate strength in short link beams are better [1]. On the other hand, the excessive reduction of the link beam length significantly increases its plastic rotation demand, and therefore the AISC seismic code [2] considers 0.08 rad limit as the maximum plastic rotation of shear link beams. In this way, the minimum allowable length for shear link beams can be calculated. Typical configurations for link beams in eccentrically braced frames are shown in Fig. 1.

1.1. Box link beams

I-shaped and box link beams are widely used in eccentrically braced frames. I-shaped link beams require lateral braces at two ends in order to prevent lateral torsional buckling due to low torsional stiffness. Unlike I-shaped link beams, box link beams do not need to insert lateral braces, provided that the moment of inertia around the weak axis is greater than 67 % of the moment of inertia around the strong axis. In places such as bridges, between the two elevator's cores and so on, where lateral braces are difficult to provide, the use of box link beams instead of I-shaped link beams is preferred. Extensive numerical and experimental studies have

* Corresponding author at: K. N. Toosi University of Technology, Civil Engineering Department, No. 1346, Vali-Asr Street, P.O. Box. 15875-4416, Tehran 19697, Iran.

E-mail addresses: fanaie@kntu.ac.ir (N. Fanaie), danial2737762@gmail.com (D. Pesaran Behbahani), samira.ebrahimi@ut.ac.ir (S. Ebrahimi).

<https://doi.org/10.1016/j.istruc.2022.11.085>

Received 29 March 2022; Received in revised form 4 October 2022; Accepted 21 November 2022

Available online 6 December 2022

2352-0124/© 2022 Institution of Structural Engineers. Published by Elsevier Ltd. All rights reserved.

Nomenclature			
b'	The pure width of the flange, regardless of the thickness of the webs	σ_{∞}^0	The maximum change in the size of the yield surface
t_f	The thickness of the flange	ϵ_{eq}^p	The equivalent plastic strain
E	The modulus of elasticity	b_f	The width of the flange in the link beam
F_{yf}	The yield stress of the flange	M_{pf}	The flange plastic moment capacity
d	The depth of the web, regardless of the thickness of the flanges	M_p	The cross-section plastic moment capacity
t_w	The thickness of the web	h_w	The depth of the corrugated plate
F_{yw}	The yield stress of the web	a	Sub-panel width
V_{ult}	The maximum shear created in the link beam	θ	The angle of wave in a corrugated plate
V_p	The nominal plastic shear capacity in link beam	β_0	The ratio of longitudinal to diagonal sub-panels width
a_0	The distance from center to center of stiffeners	τ_Y	The shear yield stress
d	The depth of the beam	$\tau_{cr,G}^e$	The elastic global buckling strength
k_z	A buckling factor	$\tau_{cr,L}^e$	The elastic local buckling strength
α_k	The Kth backstress, which represents the location of the center of the yield surface	ν	The Poisson's ratio of the steel
C_k	The initial kinematic strain hardening slope	D	The flexural elastic stiffness of the plate
γ_k	The reduction rate of the kinematic hardening slope	k_L	The local buckling factor as a function of the plate's aspect ratio and boundary conditions
ϵ^p	The Plastic strain	β	The global buckling factor as a function of the plate's boundary conditions
α_0^k	The initial size of the backstress	D_x	The flexural elastic stiffness of the corrugated plate along the x-axis
$\Delta\epsilon^p$	The difference between the plastic strain value at the beginning and end of a tensile or compressive half cycle	D_y	The flexural elastic stiffness of the corrugated plate along the y-axis
$\sigma _0$	The initial size of the yield surface	τ_n	The critical buckling strength

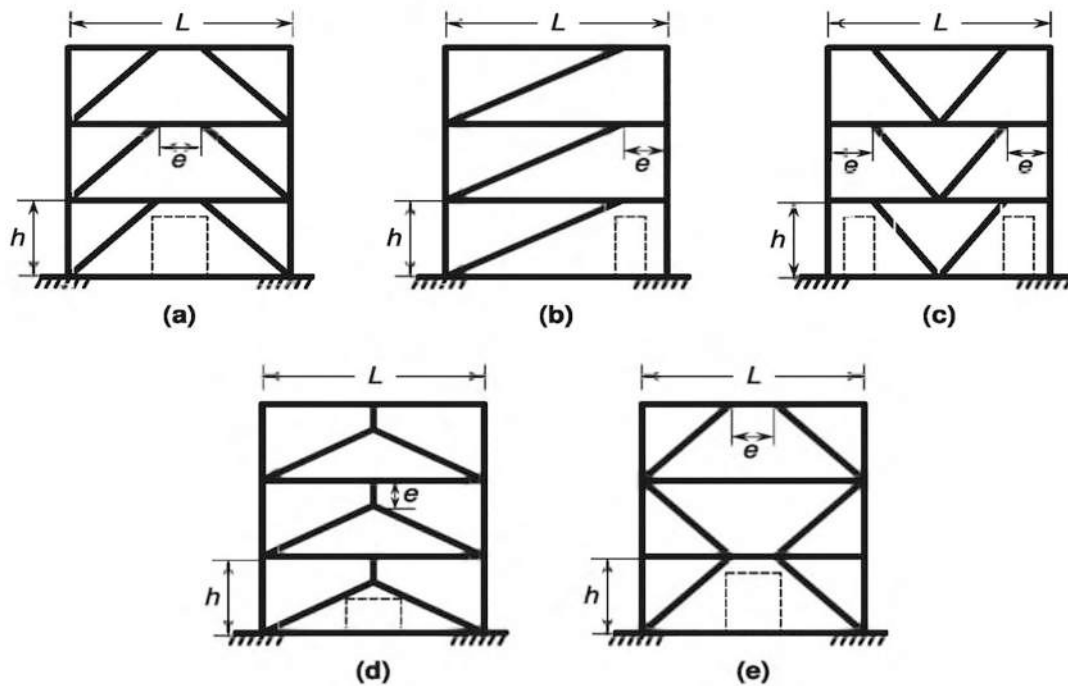


Fig. 1. Typical configurations for link beams in eccentrically braced frames [3].

investigated the behavior of I-shaped link beams; however, fewer studies have investigated the behavior of box link beams. Berman and Bruneau theoretically and experimentally examined the box link beam's behavior and presented the results below [4,5].

1.1.1. The maximum allowable compactness ratio of box link beams

Flange bucklings in link beams may lead to lateral torsional buckling,

severe strength degradation, and loss of ductility. Berman and Bruneau stated when the ratio of the average axial stresses due to the bending moment at the end of the link beam's flange to the flange material's yield stress is greater than 1.3; flange buckling is likely [4]. Therefore, to prevent flange buckling in box link beams with shear yielding behavior, they suggested a maximum value of $1.00\sqrt{\frac{E}{F_{yf}}}$ for the flange compactness



Fig. 2. Fracture in the vicinity of stiffener connection to the link beam web [7].

ratio ($\frac{b'}{t_w}$) of box link beams [4]. In addition, they suggested maximum values of $1.67\sqrt{\frac{E}{F_{yw}}}$ and $0.64\sqrt{\frac{E}{F_{yw}}}$ for the web compactness ratio of box link beams ($\frac{d'}{t_w}$), with shear yielding behavior and with or without intermediate stiffeners, respectively.

1.1.2. Over-strength factor of link beams

In eccentrically braced frames, the maximum strength of link beams is important to determine design forces in force-controlled frame members. Over-strength factor for short link beams is defined as the ratio of maximum shear force generated to the plastic shear capacity of the link beam's section. Different parameters such as strain hardening of link beam materials, the ratio of the material's expected yield stress to the material's minimum yield stress, flange participation in bearing the shear, and effects of beam and slab composite action, influence the over-strength factor in link beams. Berman and Bruneau's studies showed that the value of the over-strength factor for box link beams with shear yielding behavior was between 1.3 and 1.9 [5]; But, the AISC seismic code [2] considered the values of 1.25 and 1.4 for over-strength factor due to cyclic hardening in I-shaped and box link beams, respectively.

1.1.3. Link beam stiffeners

Kasai and Popov's [6] studies showed that under cyclic loading, short link beams without intermediate stiffeners experience strength and stiffness degradation and consequently reduced energy dissipation due to the early occurrence of plastic shear buckling in the web of link beams; Therefore, they suggested that the intermediate stiffeners should be used throughout the link beams. Their studies showed that the intermediate stiffeners of the link beam lead to delayed shear buckling of the web, and ensure stable cyclic behavior. Accordingly, Kasai and Popov suggested the equation of $\frac{a_0}{t_w} + \frac{1}{8} \frac{d}{t_w} = C_B$ with a condition of $a_0 \leq d$ for estimating the distance between the intermediate stiffeners of the I-shaped link beams where C_B is determined equal to 56, 38, and 29 for maximum link beam rotations of 0.03, 0.06, and 0.09 rad, respectively [6]. Similarly, to delay shear buckling of the webs, Berman and Bruneau proposed the formula $\frac{a_0}{t_w} + \frac{1}{8} \frac{d}{t_w} = C_B$ with a condition of $a_0 \leq d$ for maximum distance between intermediate stiffeners of the box link beam where C_B is 20 and 37 for the maximum rotation angle of the 0.08 and 0.02 rad, respectively [4]. Berman and Bruneau's studies showed that the use of intermediate stiffeners in box link beams with a web compactness ratio less than $0.64\sqrt{\frac{E}{F_{yw}}}$ is not necessary. They also stated that the use of intermediate stiffeners in link beams with a web compactness ratio greater than $1.67\sqrt{\frac{E}{F_{yw}}}$ cannot prevent web buckling [4]. Connecting the stiffeners to the link beam increases the cost and reduces the speed of construction. Studies by Lian et al. [7] showed that link beams experienced fracture in the vicinity of stiffener connection to the web of the link beam in large deformations due to stress and strain concentration in this region, and then this fracture spread deep into the

web (Fig. 2). Consequently, elimination of intermediate stiffeners in link beams can prevent stress concentration and fracture in the vicinity of stiffeners and as a result, the link beam's ductility increases.

1.2. Corrugated plates

Corrugated plates are one of the oldest types of steel produced as cold rolled and, as a result, their construction has a relatively simple and low-cost process. Wave creation with different shapes increases the out-of-plane stiffness in thin plates; In addition, the fold line in this type of plate has relatively high stiffness and similar to transverse stiffeners, it increases the buckling capacity; In fact, the geometrical properties of the corrugated plate are converted from isotropic to orthotropic state, and by changing the geometry of the plate, more strength is created by consuming less materials. Low weight, high strength, suitable out-of-plane stiffness, ease of use, easy construction, and no need for intermediate stiffeners are inherent characteristics of corrugated plates.

Elgaaly et al. [8] conducted experiments and numerical studies on I-shaped beams with corrugated web, concluding that the failure mode of the corrugated plate was global or local buckling; If the wavelengths are large, local buckling dominates the behavior of the corrugated web, and when the waves are dense and with less wavelengths, the global buckling dominates the behavior of the corrugated web [9]. Theoretically, local buckling occurs in a flat sub-panel, while global buckling consists of several sub-panels and extends diagonally throughout the entire depth of the web. They also suggested that when the critical stress of local or global elastic buckling exceeds 80 % of the material's shear yield stress, the buckling of the plate will be inelastic. Driver et al. [10] indicated that the shear strength of the I-shaped beams with a corrugated web is a function of web depth, plate thickness, wave geometry, material specifications, and initial geometric imperfection. They also stated that the corrugated web could not withstand the axial stresses (accordion effect), and it can be assumed that the flanges supply the entire bending moment of the beam and there is no need to consider the interaction between shear and flexure in the beam. According to the experiments, the observed failure mode is a combination of the two above-mentioned modes called interactive buckling mode. According to the investigations conducted by Driver et al. [10], the lowness in the ratio of longitudinal to diagonal sub-panels widths causes the design to be not cost-effective, and if this ratio is high, it reduces the critical stress of the global buckling, and the amount of this parameter according to Abbas's recommendation [11] should be between 1 and 2.

Sayed-Ahmed [12] indicated that using a corrugated web reduces the required thickness for the web plates and removes the welds related to the stiffeners, making the design lighter and more economical. He presented an equation to determine the critical interactive buckling stress for trapezoidal and zigzag corrugated webs. Using the finite element method, Yi et al. [13] realized that in the corrugated web, the failure caused by shear buckling often has the characteristics of both global and local buckling modes, called interactive buckling. Finally, they presented relationships to determine the critical buckling stress of I-shaped beams with the corrugated web. El Metwally and Loov [14] studied beams with corrugated webs and prestressed concrete flanges. They presented the advantages of using the corrugated web in the beams listed as follows: 1) reducing the stress required to prestress the flanges due to the accordion effect of the corrugated plate, 2) the possibility of increasing the beam length due to its dead load reduction, and 3) the appropriate distribution of stress between the flanges and webs, so that the flanges bear just bending and the webs bear just shear. Finally, they presented a relationship to determine the shear capacity of trapezoidal corrugated webs. Sause and Braxtan [15] studied these plates in order to evaluate the equations presented up to that time for determining the shear capacity of the corrugated plates and concluded that the assumptions intended to provide equations were not in line with the experiments conducted. In addition, they presented an equation to determine the shear strength in trapezoidal corrugated webs.

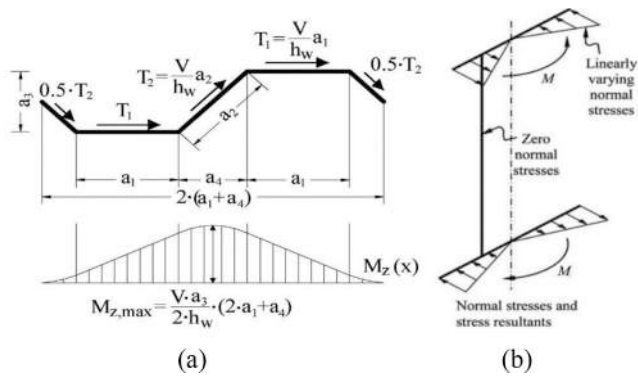


Fig. 3. The transverse moment of the flange (a) how the transverse moment changes along the beam, and (b) the transverse moment and its resulting stresses in the flange.

Nie et al. [16] studied the shear strength of composite box link beams with trapezoidal corrugated webs numerically and experimentally, and they concluded that webs were in pure shear mode. This conclusion confirms the existence of the accordion effect in the corrugated web.

Riahi et al. [17] numerically studied the I-shaped beam with flat, trapezoidal, sinusoidal, and zigzag webs. According to their studies, the shear strength of the corrugated web is about 1.5 to 2 times the strength of the web with a flat plate without stiffener and equal thickness. They noted that increasing the thickness of the flange has no significant effect on the buckling strength of the corrugated plate, but it can increase the stiffness of the beam. Elkawas et al. [18] examined the use of the corrugated web in bridge girders made of high-yield point steel. This type of beam can save weight by reducing the web thickness and eliminating transversal stiffeners (due to a higher yield point for steel and higher out-of-plane stiffness of the web plate). The decreased bending moment demand due to lesser dead loads makes it possible to use longer beams with a specified section (higher span to depth ratios). It's worth mentioning that using corrugated web reduces the beam's flexural stiffness due to the web accordion effect and also, due to lower shear modulus of corrugated webs, the shear stiffness of the beam decreases; Considering the lower stiffness of beams with corrugated webs, the deformation demands may limit the maximum length of the beam. Elkawas et al. [18] presented a relationship to calculate critical shear stress, given the ratio of sub-panel width to the depth of web in beams with trapezoidal corrugated webs ($\frac{d}{h_w}$). They also expressed that unlike conventional plate girders with flat webs which exhibit plastic hinges when the developed diagonal tension field yields, plastic hinges do not form in girders with corrugated web plates failing by local and interactive buckling modes and suggested a wave angle value greater than 30° to avoid domination of the global buckling mode. Leblouba et al. [19] experimentally studied the behavior of beams with corrugated webs. Following Leblouba's studies, the post-buckling (residual) strength of tested beams with the corrugated web is not significantly influenced by the mode of shear buckling and is estimated to be around

50 % of their ultimate load-carrying capacity. In addition, Leblouba et al. investigated previously published analytical models for the estimation of the shear strength of trapezoidal corrugated webs and developed a new model. Their model is shown to be more accurate than previously published models for estimating the shear strength of corrugated steel webs, allowing for more economical designs. Since the shear strength of corrugated webs is a function of several geometric parameters, Leblouba et al. [20] performed a sensitivity analysis to estimate each parameter's relative contribution to the shear strength behavior. The study showed that the width of the flat folds and web thickness are the most influential parameters on the shear strength of corrugated webs, followed by the web height. Other geometrical parameters such as the wave angle (in the range of 30° to 45°) and The ratio of longitudinal to diagonal sub-panels width (in the range of 0.8 to 3) have less impact on the shear strength.

In general, the designing shear strength of corrugated plates is less discussed in design regulations. Among the limited regulations, Eurocode 3 [21] provides equations to determine the shear strength of steel girders with the corrugated web.

Lho et al. [22] investigated the behavior of beams with a thinner-than-usual corrugated web used in industrial structures. They defined the compactness ratio of corrugated webs as $0.8 \left(\frac{d}{h_w}\right) \sqrt{\left(\frac{F_{yw}}{E}\right) \left(\frac{1}{k_c}\right)}$ and stated that if the corrugated web compactness ratio is more than $0.474 \sqrt{\frac{E}{F_{yw}}}$, vertical buckling of flanges occurs.

According to Abbas's studies [23], I-shaped beams with corrugated webs, experience in-plane deformations and out-of-plane torsion under an in-plane moment and shear. Out-of-plane torsion can be considered as the transverse flange moment (Fig. 3a). Transverse moment in the flange of the I-shaped beam with a corrugated web adds to the axial stresses caused by the in-plane bending. The transverse moment occurs due to the presence of shear flow in the web and the eccentricity of this flow relative to the beam center line. To determine the transverse moment in the flange, they presented a method known as the Fictitious Load Method. Kovsdi et al. [24] also studied the transverse moment of the flange in I-shaped beams with a corrugated web. According to their research, the amount of this moment varies along the beam length (Fig. 3b).

Local buckling of flanges with the corrugated web was investigated by Cafolla [25]. They indicated that by increasing the ratio of the width of sub-panels to larger flange outstand and keeping total flange width, the critical stress of the flange buckling decreases. Li et al. [26] examined the local flange buckling of the beams with the corrugated web and presented a relationship for the maximum compactness ratio of the flange in order to prevent its buckling before yielding.

Sherman and fisher [27] investigated the connectivity between the corrugated web and flanges to determine how much connection is needed between the flanges with a corrugated web to develop a full yield strength. Their experiment results indicated that connecting the diagonal panels has a negligible effect on the stiffness and strength of the beam under monotonic loads and with a corrugation wave angle larger than 45° . They reported two basic types of web-to-flange connection



Fig. 4. Cracks caused by cyclic loading in beam with corrugated web [29].

failure: a) tearing of web material, b) failure through the throat of solder fillet or the fillet bond. As the length of the fillet weld decreases, the force concentration may cause the web to tear in shear along the toe of the fillet. Elamary et al. [28] studied the failure mechanism of hybrid steel beams with trapezoidal corrugated web and non-welded inclined folds to eliminate the possibility of failure due to the propagation of fatigue cracks initiated near the ends of inclined sub-panels. Their tests showed that corrugated webs with non-welded inclined sub-panels failed due to the web tearing. Finally, Elamary et al. [28] concluded that the ultimate load-bearing capacity of corrugated webs with non-welded inclined folds is less than fully welded webs (with failure mode of fatigue cracks propagation). Ibrahim et al. [29] conducted studies to investigate the fatigue behavior in I-shaped beams with corrugated webs (continuously welded to the flanges) under cyclic loading and indicated that the fatigue life of a beam with a corrugated web is about 28 % to 53 % higher than that of a flat web with stiffeners. They also found that two factors affecting the fatigue life of I-shaped beams with corrugated web are the angle of the wave and fillet radius between the sub-panels. According to this research, under cyclic loading in beams with corrugated web, cracks start in the vicinity of the weld of the web to the flange (Fig. 4). Ibrahim et al. [29], in order to reduce stress concentration and increase the fatigue life of beams with corrugated webs, suggested that the fillet radius between sub-panels should be equal to a quarter of the radius of the escribed circle in the wave.

Shahmohammadi et al. [30] investigated the steel coupling beams with corrugated webs and found that the rotational capacity of the coupling beams increased by increasing the angle of the waves, increasing the number of half waves at a specified length, and decreasing the compactness ratio of the web plate. Also, Hajsadeghi et al. [31] studied the energy dissipation of steel coupling beams with the corrugated web. Using finite element modeling, they concluded that changing the thickness of the plate has the most significant effect on changing the amount of energy dissipation and that the impact of changing the angle of the wave and the number of half waves on the energy dissipation of the samples is less, and also that the effect of half waves on energy dissipation is greater than that of the angle of the wave.

Most of the research on using corrugated plates as the web of beams, considered the web as a forced controlled element (without undergoing inelastic deformations) under gravity loads. Other researchers have not addressed using corrugated plates as the webs of shear box link beams to increase buckling stability under cyclic loading and eliminate intermediate stiffeners; In this study, trapezoidal corrugated webs have been used for the webs of box link beams and as a structural fuse (under inelastic excursions) for the first time. Abaqus finite element software was considered to evaluate box link beams with corrugating web and without intermediate stiffeners.

2. Finite element modeling

2.1. Verification of numerical models

Abaqus software is one finite element software used to solve various engineering problems. In this study, in order to ensure the accuracy of finite element modeling in Abaqus software, three experimental studies were selected: 1) a box link beam with intermediate stiffeners tested by Berman and Bruneau [5], and 2) a steel shear wall with corrugated web under cyclic loading tested by Emami et al. [32], and 3) an I beam with a trapezoidal corrugated web under monotonic loading. With regard to the corrugated web, most studies have been conducted as monotonic loading on I-shaped beams, and limited experiments have been conducted on the cyclic behavior of the corrugated web. Many studies have presented that the stress distribution in the web of the link beam is somehow similar to the behavior of the shear wall's web plate. In this way, the plate of the shear wall can be considered similar to the link beam web, columns in the shear wall can be considered identical to the link beam flanges, and beams can be considered equivalent to stiffeners

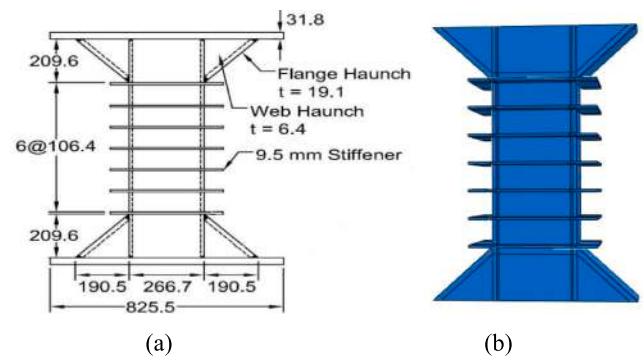


Fig. 5. Experimental specimen of X2L1.2 in Berman and Bruneau's studies (a) the dimensions of the experimental specimen [5] and (b) The modeled specimen.

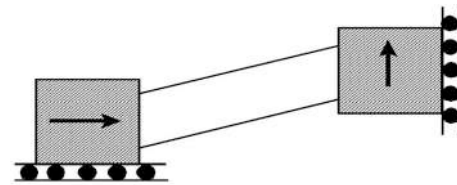


Fig. 6. Boundary conditions of link beams [5].

at the end of the link beam. Therefore, to verify the behavior of the link beam with the corrugated web under cyclic loading, the verification of the behavior of the corrugated steel shear wall has been used.

2.1.1. The first verification: Box link beam under cyclic loading

As shown in Fig. 5, the first verification was done by considering the box link specimen X2L1.2 in Berman and Bruneau's studies [5]. The specifications of this specimen are flange thickness of 12.7 mm, web thickness of 6.4 mm, a total width of 209.6 mm, depth of 266.7 mm, stiffener width of 66.7 mm, and stiffener thickness of 9.5 mm. This link beam has a shear yielding behavior with a normalized length of 1.2.

In the experimental studies of Berman and Bruneau [5], haunches were inserted at the two ends of the link beam to gradually change the cross-section and prevent fracture at the two ends of the link beam and in their flanges. In order to consider rotational degrees of freedom in nodes, 8-node incompatible solid elements (C3D8I), which have modified formulations compared to 8-node with reduced integration solid elements (C3D8R), were used. Different studies have presented different values to determine the size of plate geometric imperfections. EN-1993-1-5 code [21] considers the value of 1/200 of the smallest dimension of the plate as the size of the initial geometric imperfections. Also, the primary modes of elastic buckling (eigenvalue analysis) are often used as forms of geometric imperfections.

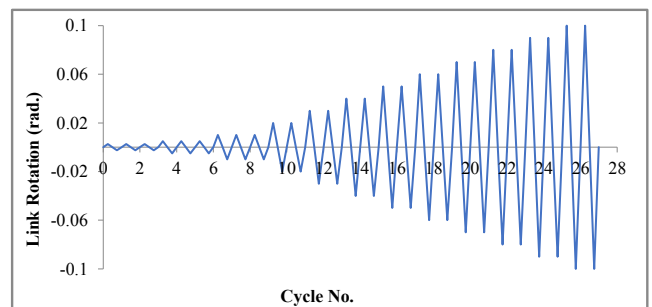


Fig. 7. Loading protocol used for verification.

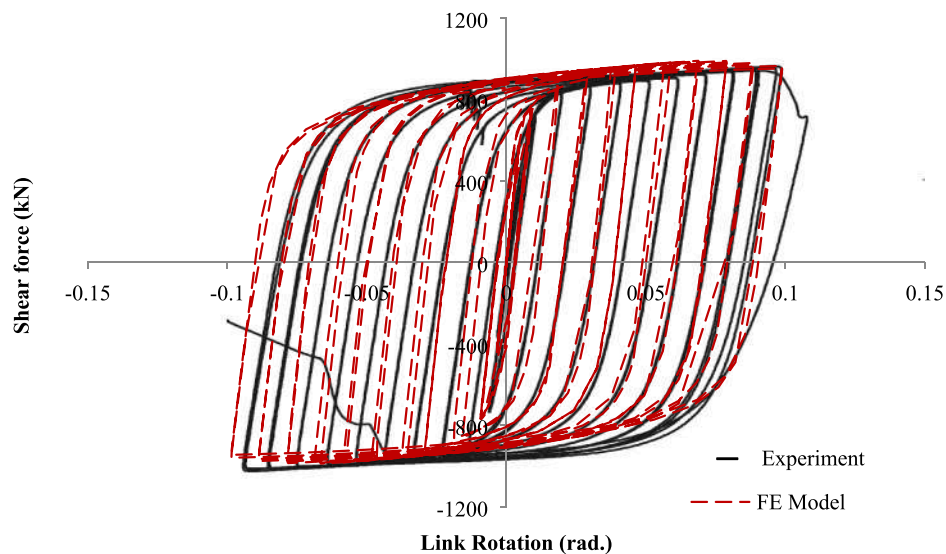
Table 1
Combined hardening parameters of web and flange.

	X2L1.2 Sample web	X2L1.2 Sample Flange
C_1 (MPa)	42,900	29,100
C_2 (MPa)	4500	1596
C_3 (MPa)	680	187
γ_1	600	300
γ_2	90	13.3
γ_3	2	1.7
σ_{l0} (MPa)	345	345
σ_{∞}^0 (MPa)	22	50
b	5.4	2

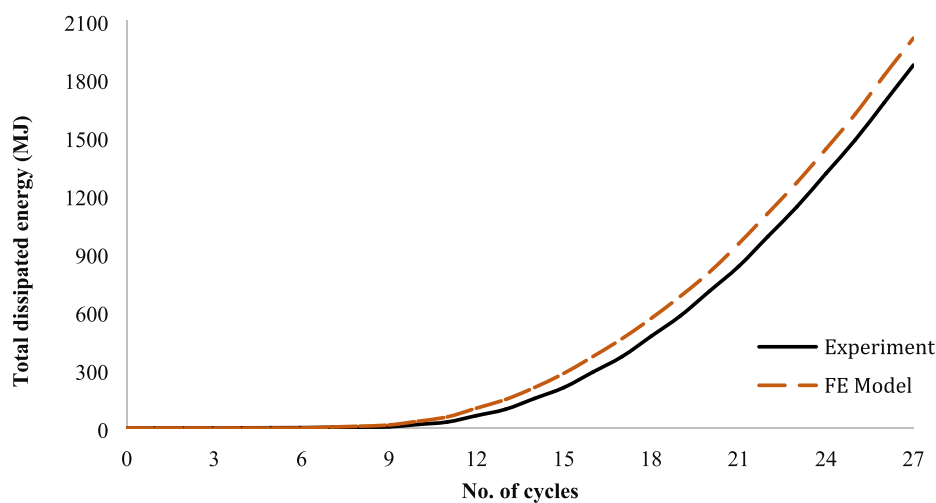
2.1.1.1. Boundary conditions and loading. The present study considered the boundary conditions proposed by Bremen and Bruneau [5] for link beams (Fig. 6). Fig. 6 shows that all rotational degrees of freedom are clamped at the two ends of the link beam. The axial transitional degree of freedom is free at one end of the link beam to prevent the creation of axial force in the link beam. In addition, the transitional degree of freedom perpendicular to the longitudinal axis of the link beam is free at

the other end of the link beam in order to apply the displacement-controlled loading to the specimen in accordance with the AISC 2002 [33] loading protocol, as shown in Fig. 7.

2.1.1.2. Materials specifications. The behavior of materials used in structural members severely affects the seismic performance of structures. The modulus of elasticity, density, and Poisson’s ratio of the steel used in all specimens is defined as 200 GPa, 7850 kg/m³ And 0.3. Link beams are expected to be able to withstand large cycle plastic deformations. In order to determine the yield of isotropic materials (such as steel) under multi-axial loading conditions, the von-Mises yielding criterion is used. This study considered using the Chaboche [34] combined hardening model (a combination of yield surface behaviors in isotropic and kinematic hardenings) because of its high accuracy in modeling strain hardening in steel. Chaboche [34] presented a nonlinear kinematic hardening model for determining backstress values as Eq. (1); Also, they suggested Eq. (2) for determining the size of the yield surface (Isotropic hardening).

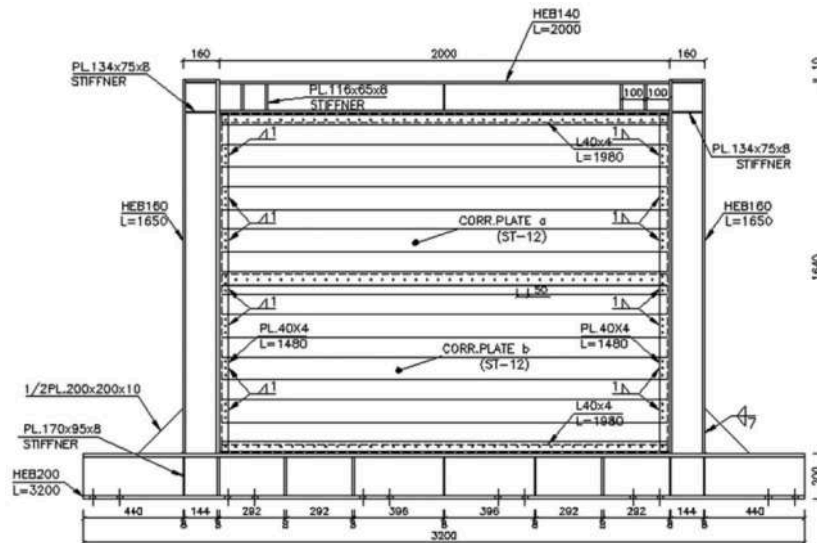


(a)

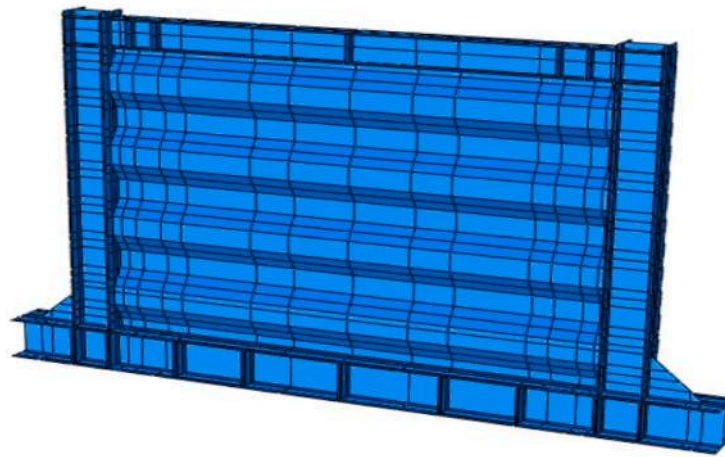


(b)

Fig. 8. Comparison between experimental and modeled specimens (a) hysteresis curves (b) total dissipated energy.



(a)



(b)

Fig. 9. Steel shear wall specimen in Emami et al.’s studies: (a) specimen’s front view and (b) FE Model in Abaqus.

$$\alpha = \sum_{k=1}^n \alpha^k = \sum_{k=1}^n \frac{C_k}{\gamma_k} [1 - e^{-\gamma_k \epsilon^p}] + \alpha_0^k e^{-\gamma_k (\epsilon^p)} \quad (1)$$

$$\sigma^0 = \sigma|_0 + \sigma_\infty^0 (1 - e^{-b\epsilon_{eq}^p}) \quad (2)$$

Note that values 0 and $-\frac{C_k}{\gamma_k} \left(\frac{1 - e^{-\gamma_k \Delta \epsilon^p}}{1 + e^{-\gamma_k \Delta \epsilon^p}} \right)$ are considered for α_0^k in monotonic and cyclic loading, respectively. The necessary parameters

Table 2
Specifications of steels used in beams, columns, and web of steel shear wall in Emami et al.’s studies.

Member	Steel type	Young’s modulus (GPa)	Yield stress F_y (MPa)	Ultimate stress F_u (MPa)	Ultimate strain (%)
Plate of shear wall	ST-12	200	207	290	41
Column	ST-44	200	300	443	33
Beam	ST-44	200	288	456	37

for modeling Chaboche combined hardening are calibrated similarly to the process described in Behbahani and Fanaie’s study [35] and presented in Table 1.

Finally, Fig. 8 shows the comparison between experimental and finite element modeling hysteresis curves and the total strain energy generated in the link beam.

2.1.2. The second verification: Steel shear wall with corrugated web under cyclic loading

The specimen was selected from Emami et al.’s [32] studies. Their experimental specimen was half-scale compared to the actual sample in the structure. Fig. 9 shows the specifications and geometric dimensions of the steel shear wall used in Emami et al.’s [32] studies.

This specimen’s columns were designed with IPB160, the upper beam with IPB140, and the floor beam with IPB200. The overall dimensions of the corrugated plate in the shear wall were 1480×1980 mm and the thickness of the plate was 1.25 mm. In the specimen, the connection of the beam to the column was implemented as rigid using a full penetration groove weld on the flanges of the beam and a fillet weld in the web. Bolts tie the beam to the bottom of the laboratory. In

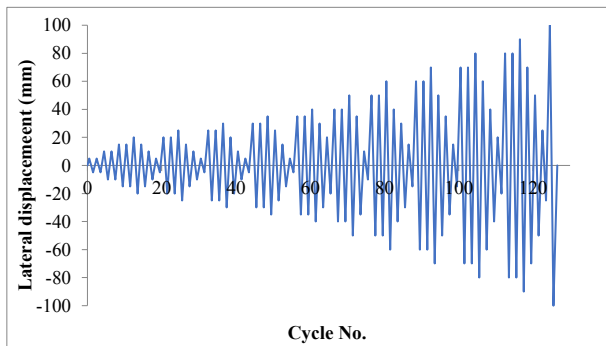


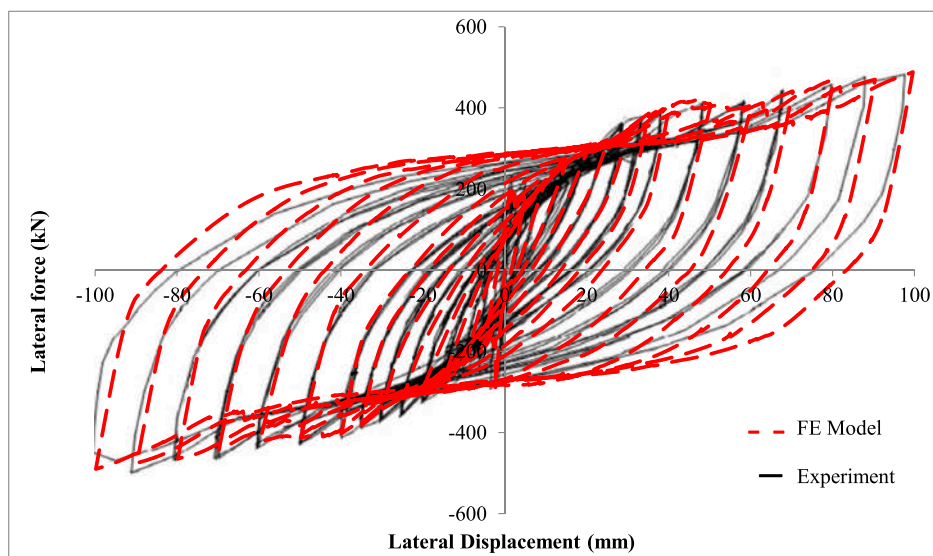
Fig. 10. Loading protocol applied to steel shear wall in Emami et al.'s study.

addition, to prevent the out-of-plane movement of the frame, two transverse beams attached to the upper beam were used as lateral braces. The specifications of the steels used in the beams, columns, and

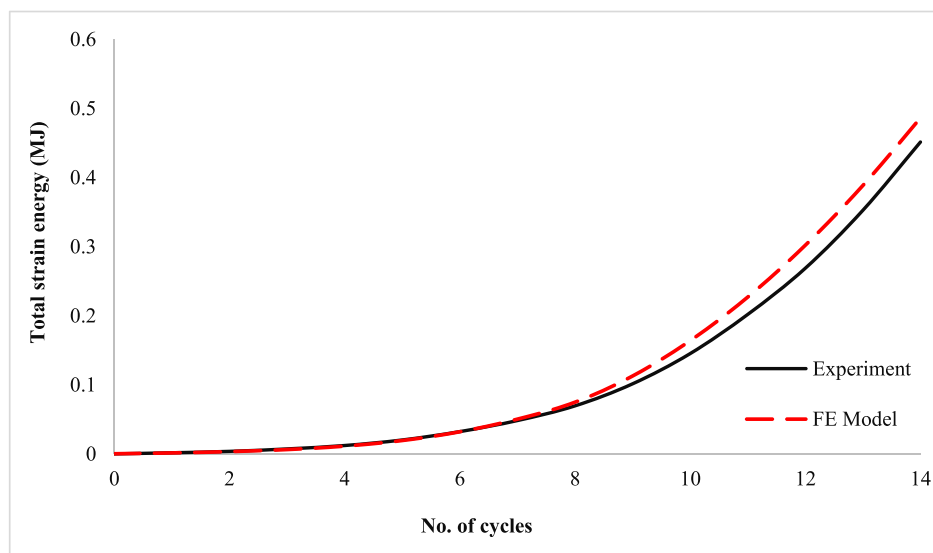
web of steel shear wall are presented in Table 2.

The static general analysis method was used in this study by adding viscose damping to prevent convergence errors. Also, in this section, S8R5 shell elements were used to model the steel members. S8R5 shell elements have eight nodes in each element, and there are five degrees of freedom in each node, including three degrees of transitional freedom and two degrees of rotational freedom. In order to improve the modeling accuracy, at least four elements were used throughout the width of each flat sub-panel in the corrugated web. In addition, initial geometric imperfections in corrugated web obtained using Eigenvalue Analysis were entered by coding in Abaqus software. The specimen's boundary conditions, similar to the test setup, were considered in the modeling. Quasi-static loading is also applied in accordance with AC 154 loading protocol [36] as a displacement-control to the upper beam. The AC 154 loading protocol is displayed in Fig. 10.

In order to make the figure simpler and increase the possibility of a better comparison, the hysteresis curves and total strain energy of experimental and modeled specimens are presented by eliminating the

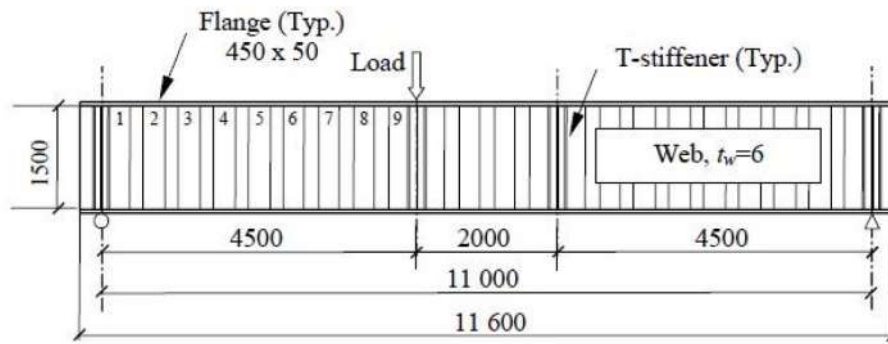


(a)

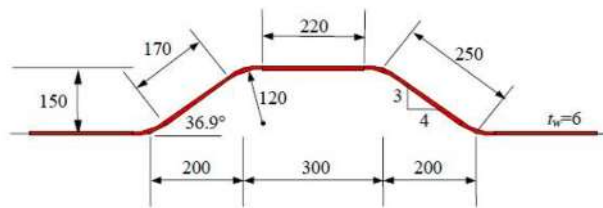


(b)

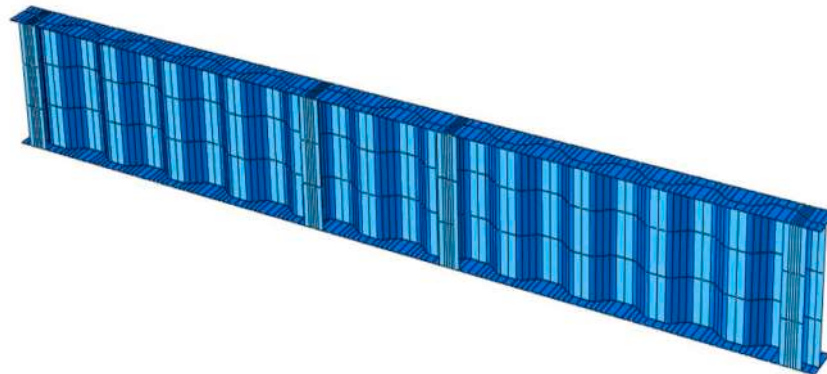
Fig. 11. Comparison of experimental and modeled specimens (a) hysteresis curves (b) total dissipated energy.



(a)



(b)



(c)

Fig. 12. Driver et al. test (a) total beam dimensions (b) corrugation geometry (c) Abaqus model.

cycles with the repetitive amounts of displacement in Fig. 11.

2.1.3. The third verification: I beam with a trapezoidal corrugated web under monotonic loading

In order to further verify FE models with corrugated web plates, a simply supported I-shaped beam with a trapezoidal corrugated web under a single concentrated monotonic load (G8A sample tested by Driver et al. [10]) is considered. In this sample, HPS 485 steel (with a yield stress of 485 MPa) has been used for the flanges and web of the beam. This type of steel has low strain hardening, so its behavior can be considered elastic-perfectly plastic. The geometric dimensions of the mentioned test setup, the corrugation dimensions, and the FE model are shown in Fig. 12.

The web thickness and height were 6 mm and 1500 mm, respectively and the flanges dimensions were 450×50 mm. In order to prevent vertical buckling of the flange in the web under concentrated load, T-shaped stiffeners are used. Also, to prevent lateral movement of the beam, two lateral braces are provided at the two ends of the beam and one 700

mm away from where the concentrated load is applied. S8R5 elements are used for modeling purpose.

Driver et al. [10] measured the maximum geometric imperfection of the corrugated web as 5.72 mm. So, initial geometric imperfection has been considered in the model by conducting an Eigenvalue analysis and in accordance with the buckling modes of the corrugated web. Static general with adding viscose damping is used for the analysis to avoid convergence problems. Finally, the FE modeling's force-displacement diagram (at the position of load application) is compared to the experimental result as shown in Fig. 13.

From Fig. 7, Fig. 10 and Fig. 13, it can be concluded that the results of Abaqus have excellent agreement with the results obtained from the two experimental studies. As a result, the modeling performed in Abaqus is acceptable.

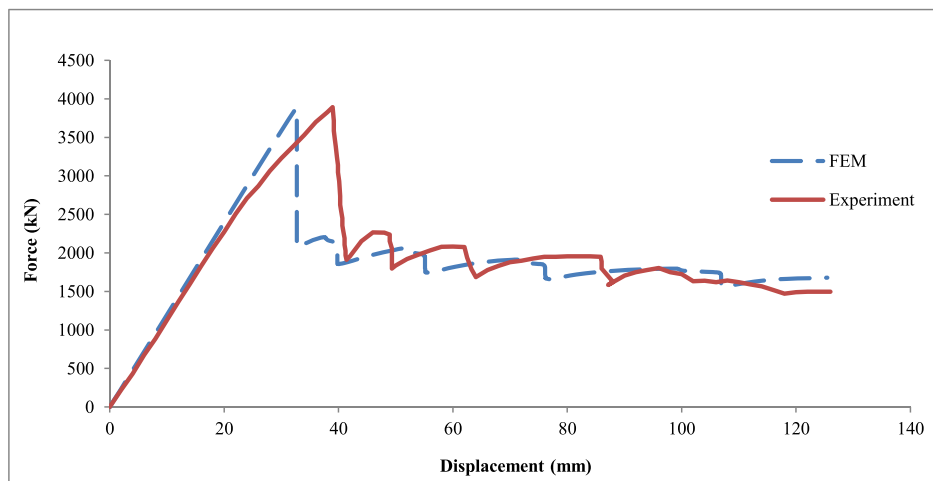


Fig. 13. Comparison of experimental and modeled specimens.

3. Using corrugated plate in webs of box link beam to eliminate intermediate stiffeners

3.1. Introducing the specimens of box link beams used in the numerical study

The most important geometric parameters affecting the buckling behavior of the corrugated plate are the width of the sub-panels, the thickness of the web plate, the depth of the web, the angle of the wave, the fillet radius between the longitudinal and diagonal sub-panels, and the ratio of the width of longitudinal to the diagonal sub-panels. In this study, the ratio of the width of sub-panels parallel to the longitudinal axis to diagonal sub-panels is assumed to be equal to 1 in accordance with Abbas et al.'s [11] recommendation, and also the fillet radius between longitudinal and diagonal sub-panels is considered equal to one-quarter of the radius of the escribed circle in a trapezoidal wave following Ibrahim et al.'s [29] studies to reduce stress concentration and increase fatigue life under cyclic loading.

This study investigates three parameters: wavelength, web compactness ratio ($\frac{h_w}{t_w}$) and the angle of the wave (θ). In the study of the web compactness ratio, both the web's depth and thickness can be changed. Shear yielding behavior was assumed for all specimens with the trapezoidal corrugated web. In addition, the length of the link beam and the net area of the web in all link beams were considered 648 mm and 1544 mm², respectively, similar to the X2L1.2 specimen. The steels used for the flanges and webs were identical to the flanges and webs materials of the X2L1.2 link beam in the experimental study of Berman and Bruneau [5].

Corrugated plates with a compactness ratio between 56 and 400 are often used in the web of steel girders under gravity loads where we do not expect significant inelastic behavior. However, studies have shown that the use of web compactness ratios of more than 56, due to the creation of large inelastic deformations in the web, leads to inappropriate cycle behavior in the web of link beams. For this reason, this study assumed the value of 45 as the maximum value for the compactness ratio of the web of the link beam. It is worth noting that according to Berman and Bruneau's studies [5], the maximum web compactness ratio in box link beams with the flat web made of A572 Gr50 steel to remove the intermediate stiffeners should be equal to 15.4. The maximum permissible compactness ratio of the web is limited to 40, even when transverse stiffeners are used.

Lindner and Huang [37] suggested a minimum wave angle of 30° to enable the sub-panels to create suitable boundary conditions and support each other in the contact area to develop appropriate local buckling capacity. In this research, by changing the dimensional ratios used in the

web of box link beams compared to the bridge's girders with the corrugated web, converting the buckling mode from the global buckling to the local buckling is achieved with larger quantities of the angle of the wave. Therefore, the wave angles between 30° and 90° were investigated in this study.

In order to parametrically investigate the effect of changes in different factors, the number of waves throughout the length of link beams was assumed to be variable between 2 and 6. Also, values of 25, 30, 35, 40, and 45 for the web compactness ratio and values of 30°, 40°, 50°, 60°, 70°, 80°, and 90° for the angle of the wave (θ) were considered. It is worth noting that due to assuming the constant amount for the link beam length, the width of the sub-panels (a) is determined according to the number of trapezoidal waves throughout the link beam and the wave angle. According to the preliminary study, by changing the flange compactness ratio ($\frac{b_f}{t_f}$) of the link beam from 17 to 24, the behavior of the link beam does not change significantly; therefore, in this study, only the results related to the flange compactness ratio of 17 were presented.

In research studies conducted on girders with the corrugated web in bridges, in order to prevent sudden global buckling, the ratio of the width of sub-panels to the depth of the web ($\frac{a}{h_w}$) is suggested between 0.1 and 0.2; the mentioned limitation results in a significant decrease in the width of the sub-panels. By reducing the width of the sub-panels, it is not possible to meet the minimum ratio of wave depth to the plate thickness ($\frac{h_w}{t_w}$), which is suggested to be greater than 10, according to Easley and McFarland's studies [38]. According to all mentioned limitations, in this study, the ratio of sub-panels width to web depth is between 0.1 and 0.7 and the ratio of wave depth to plate thickness is changed between 1.8 and 18.96.

In order to name the specimens, first, the letter C is used for showing the link beams with corrugated web, then the amount of web compactness ratio ($\frac{h_w}{t_w}$), the flange compactness ratio ($\frac{b_f}{t_f}$), the number of waves in the link beam length and the angle of the wave (θ) are presented, respectively. It is worth noting that due to the accordion effect, the bending capacity of the corrugated web in the link beam is excluded, and the bending capacity of the link beam with the corrugated web is determined from Eq. (3). In this study, the maximum moment value at the end of the link beam was limited to 1.2 times the plastic moment capacity of the cross-section.

$$M_{Pf} = M_p = F_{yf} \cdot b_f \cdot t_f (d - t_f) \tag{3}$$

The values of web thickness, web depth, flange thickness and flange width of specimens with different web compactness ratios are presented in Table 3.

Driver et al. [10], in order to prevent the global buckling mode

Table 3
Webs and flanges characteristics of specimens with flange compactness ratio equal to 17.

Web compactness ratio $\frac{h_w}{t_w}$	Web thickness $t_w(mm)$	Web depth $h_w(mm)$	Flange thickness $t_f(mm)$	Flange width $b_f(mm)$
25	7.85	196.48	14.53	262.71
30	7.17	215.24	13.96	251.66
35	6.64	232.4	13.49	242.61
40	6.21	248.54	13.09	234.95
45	5.86	263.61	12.75	228.47

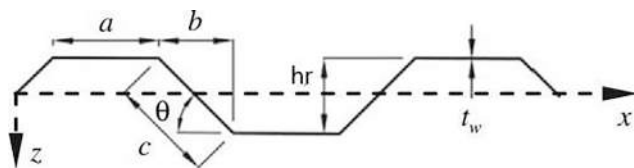


Fig. 14. Geometric parameters of the trapezoidal corrugated web.

before local buckling, limited the maximum web compactness ratio of the link beams according to Eq. (4).

$$\frac{h_w}{t_w} \leq 1.91\psi \sqrt{\frac{E}{F_y} \left(\frac{a}{t_w}\right)^{1.5} F(\theta, \beta_0)} \tag{4}$$

where ψ is a safety factor, which is often assumed to be 0.9 and $F(\alpha, \beta_0)$ is defined as Eq. (5).

$$F(\theta, \beta_0) = \sqrt{\frac{(1 + \beta_0)\sin^3\theta}{\beta_0 + \cos\theta} \left\{ \frac{3\beta_0 + 1}{\beta_0^2(\beta_0 + 1)} \right\}^{3/4}} \tag{5}$$

Moon et al. [39] presented the inequality in Eq. (6) to buckle the corrugated plates after the plate yield (in the girder of the bridges).

$$1.1 \left[\frac{5.34 \left(\frac{h_w}{t_w}\right)^{-1.5} \left(\frac{h_w}{t_w}\right)^2 + 5.72 \left(\frac{a}{t_w}\right)^2}{30.54} \right] \frac{\tau_y}{E} \leq 0.36 \tag{6}$$

The geometric parameters used in these equations are shown in Fig. 14. It is worth noting that the geometry of trapezoidal corrugated plates used in the web of link beams in this study satisfies the limitations mentioned above.

3.2. Parametric investigation on the behavior of box link beams with trapezoidal corrugated web

In this study, the introduced specimens were modeled in Abaqus software. Due to the small thickness of plates compared to their other dimensions, S8R5 elements were used. The dimensions of the used elements are also determined in such a way that there are at least four elements in the width of each sub-panel, and the aspect ratio of the elements is smaller than 2. In order to consider the geometric imperfections in the specimens, first, an Eigenvalue analysis was performed to determine buckling modes; then, according to the carried-out studies, the imperfection size was considered to be 1/200 of sub-panel width. Based on the Eigen Buckling Analysis, three modes of local, global, and interactive buckling were observed in the specimens. These three buckling modes are shown in Fig. 15.

4. Results

4.1. Determination of the slenderness ratio of the corrugated web in the box link beams

In the link beams with corrugated web, in addition to the web's compactness ratio, the wave's angle and width of the sub-panels are also involved in calculating the critical elastic shear buckling and the web slenderness ratio. According to various studies such as Sause and

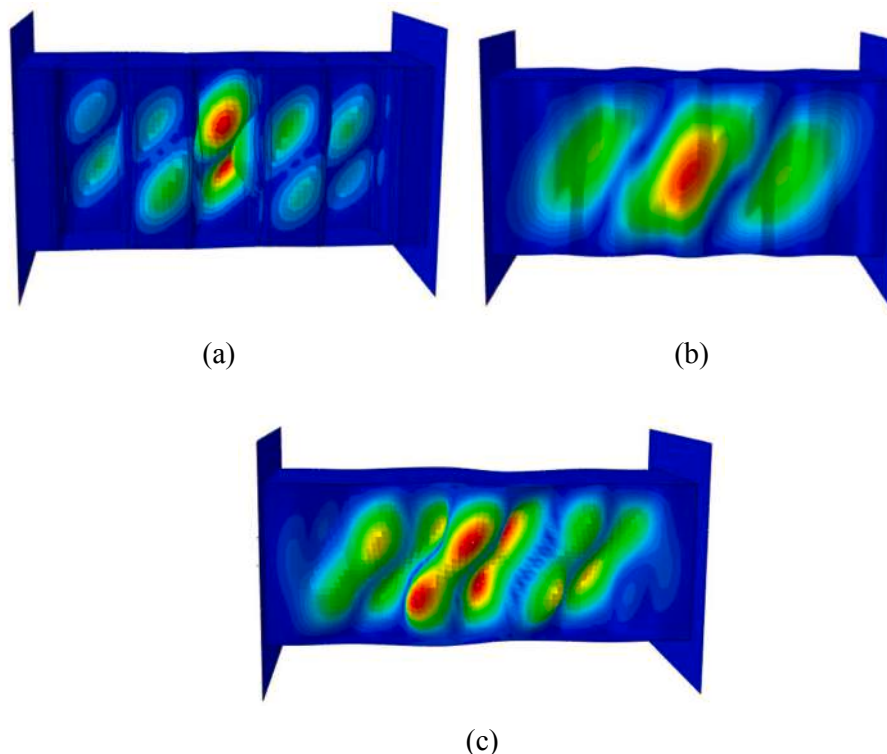


Fig. 15. Types of shear buckling observed in webs of link beams: (a) local shear buckling, (b) global shear buckling, and (c) interactive shear buckling.

Braxtan’s research [15], the slenderness ratio of corrugated plates is obtained in accordance with Eq. (7).

$$\lambda_s = \sqrt{\frac{\tau_Y}{\tau_{cr}^e}} \tag{7}$$

The critical stress of elastic shear buckling in corrugated plates was presented by different researchers as the general form of Eq. (8). It should be noted that the researchers presented different values for the n parameter.

$$\left(\frac{1}{\tau_{cr}^e}\right)^n = \left(\frac{1}{\tau_{cr,L}^e}\right)^n + \left(\frac{1}{\tau_{cr,G}^e}\right)^n \tag{8}$$

In order to investigate the adaption of theoretical equations to determine the critical elastic shear buckling stress in the web of link beam, this parameter was determined by Eigenvalue Analysis in Abaqus software. Then the critical stresses of global and local elastic buckling were calculated according to the existing theoretical relationships. Similar to the critical stress of flat plates, the critical stress of sub-panels buckling is obtained from Eq. (9) proposed by Timoshenko and Gere [40].

$$\tau_{cr,L}^e = k_L \frac{\pi^2 D}{t_w a^2} = k_L \frac{\pi^2 E}{12(1 - \nu^2) \left(\frac{a}{t_w}\right)^2} \tag{9}$$

According to Hassanein and Kharoob’s studies [41], if the ratio of flange thickness to web thickness in beams is greater than 3, the boundary conditions of the sub-panels should be considered as rigid at the junction to the flange and as simple at the fold lines of the sub-panels; Thus, the local buckling coefficient can be calculated from the Eq. (10).

$$K_L = 5.34 + 2.31 \left(\frac{a}{h_w}\right) - 3.44 \left(\frac{a}{h_w}\right)^2 + 8.39 \left(\frac{a}{h_w}\right)^3 \tag{10}$$

In this study, if the ratio of flange thickness to web thickness is 1, the sub-panels boundary conditions are assumed as simple on all edges, and the local buckling coefficient is determined according to Eq. (11).

$$K_L = 5.34 + 4 \left(\frac{a}{h_w}\right)^2 \tag{11}$$

If the ratio of flange thickness to web thickness is between 1 and 3, interpolation can be used to obtain the local buckling coefficient.

Easley and McFarland [38], assuming that the corrugated plate can be analyzed as an orthotropic flat plate with constant thickness, provided relationships to determine the global shear buckling capacity. To determine the critical stress of global buckling, Eqs. (12) – (14) were used.

$$\tau_{cr,G}^e = 36\beta \frac{(D_y D_x^3)^{1/4}}{t_w h_w^2} \tag{12}$$

$$D_y = \frac{E t_w^3}{12(1 - \nu^2)} \left(\frac{a+b}{a+c}\right) \tag{13}$$

$$D_x = \frac{E t_w^3 \left[\left(\frac{h_c}{t_w}\right)^2 + 1\right]}{6 \left(\frac{a+b}{a+c}\right)} \tag{14}$$

Using the above relationships to determine the critical stress of local and global buckling, and calculating the critical stress of interactive buckling with n values equal to 1, 2, 3, and then comparing those with the results of Abaqus software presented in Table A1, it was found that the use of interaction relationship with n value equal to 1 and β equal to 1.3 gives the best results. The mean and standard deviation values of slenderness ratios with different values of β and n obtained from modeling in Abaqus software are presented in Table 4.

In general, by reducing the link beam web’s compactness ratio, the

Table 4
Determining appropriate assumptions for calculation of λ_s .

	$n = 1$		$n = 2$		$n = 3$	
	$\left(\frac{\lambda_{s,eq}}{\lambda_{s,FEA}}\right)_{Ave}$	$\left(\frac{\lambda_{s,eq}}{\lambda_{s,FEA}}\right)_{SD}$	$\left(\frac{\lambda_{s,eq}}{\lambda_{s,FEA}}\right)_{Ave}$	$\left(\frac{\lambda_{s,eq}}{\lambda_{s,FEA}}\right)_{SD}$	$\left(\frac{\lambda_{s,eq}}{\lambda_{s,FEA}}\right)_{Ave}$	$\left(\frac{\lambda_{s,eq}}{\lambda_{s,FEA}}\right)_{SD}$
$\beta = 1$	1.07	0.11	0.97	0.14	0.95	0.15
$\beta = 1.3$	1.01	0.08	0.91	0.11	0.89	0.12
$\beta = 1.6$	0.96	0.07	0.87	0.1	0.85	0.11
$\beta = 1.9$	0.93	0.07	0.84	0.1	0.83	0.11

web’s slenderness ratio is decreased regardless of the amount of the other two parameters. Still, the way the slenderness ratio changes by changing the angle of the wave and the number of waves in the link beam length (especially the angle of the wave) have an uncertain trend. Its increase or decrease depends on the amount of two other parameters. How slenderness changes with the mentioned geometric parameters is shown in Fig. 16.

4.2. Investigation of inelastic buckling capacity of box link beam with corrugated web under monotonic loading

Considering that occurrence of inelastic deformations is expected in the link beam web, in this section, the change of inelastic buckling strength of box link beams with corrugated web under monotonic loading was discussed. According to the results presented in Table A1 of Appendix A, increasing the wave angle and reducing the compactness ratio increase the shear capacity of the cross-section. Still, the number of waves throughout the link beam does not have a specific trend on the inelastic shear capacity of the corrugated web. By increasing the number of waves in the webs of link beams, the inelastic buckling capacity of the web rises first, but then with its further increase, the critical inelastic buckling stress decreases (Fig. 17).

Various researchers have presented several equations to determine the inelastic capacity of shear buckling in the web of steel girders under monotonic loading. The results of this study indicated that the critical inelastic buckling stress shows a considerable dispersion. Still, using the equation proposed by Sause and Braxtan [15] (Eq. (15)), and assuming $n = 1$ in the interaction equation and u equal to 0.52, it is possible to estimate a lower band value of critical inelastic buckling stress (90% of the FE results have bigger critical inelastic buckling strength than the equation presented) in the web plate of box link beams. Eq. (15) can also be rewritten as Eq. (16) in terms of web slenderness ratio.

$$\tau_n = \left(\frac{1}{(\tau_{cr,L}^e)^n} + \frac{1}{(\tau_{cr,G}^e)^n} + \frac{u}{(\tau_Y)^n}\right)^{-1/n} \tag{15}$$

$$\tau_n = \tau_Y \left(\frac{1}{\lambda_s + 0.52}\right) \tag{16}$$

Fig. 18 shows the comparison between critical inelastic shear buckling stress versus slenderness ratio of the corrugated plate for Eq. (16) and the results of modeling.

4.3. Behavior of box link beams with corrugated webs under cyclic loading

4.3.1. Investigation of hysteresis curves of box link beams

In this section, the behavior of link beams was investigated under cyclic loading because link beams are cyclically loaded in earthquakes. It should be noted that following the studies of Richards and Uang [42], the loading protocol for link beams, which is available in AISC 2002 [33], imposes an equivalent plastic strain of about 60% more than the actual limit in a real earthquake for short link beams; Therefore, to load

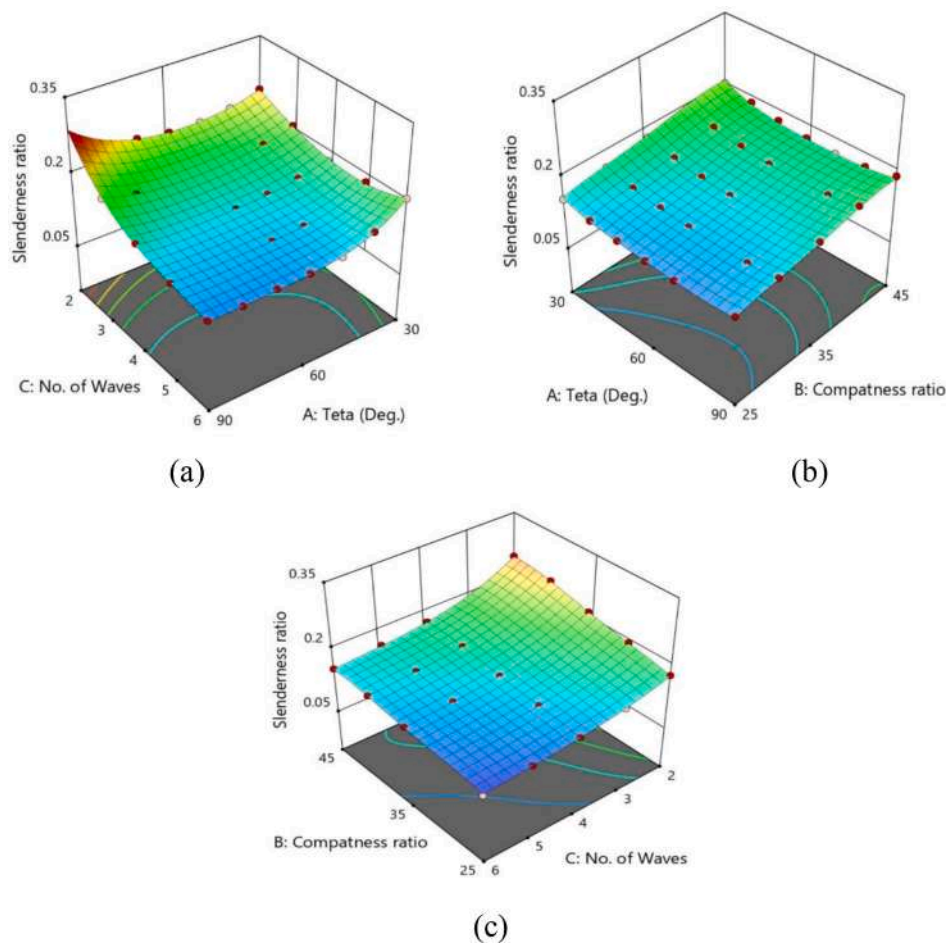


Fig. 16. How the slenderness ratio of the corrugated web changes with: (a) the compactness ratio of the web plate equal to 35, (b) 4 waves in the length of the link beam, and (c) the wave angle of 60°.

the box link beam specimens with corrugated webs, the modified loading protocol for the link beams proposed by Richards and Uang [42] was used. At first, in order to qualitatively compare, hysteresis curves of the link beam specimens with corrugated webs were compared with the X2L1.2 specimen of Berman and Bruneau [5]. Due to the large number of modelings performed in this study, only hysteresis curves for eight samples modeled in Abaqus software are shown in Fig. 19. It is worth noting that the fracture in the X2L1.2 specimen caused the test to stop, but the fracture was not considered in the modeling performed in this section. From the comparison of hysteresis diagrams, it can be concluded that in general, by decreasing the web’s compactness ratio and increasing the wave’s angle and the number of waves throughout the link beams, shear buckling in the web of link beams is delayed. Thus the stiffness and strength degradation occurs in a larger rotation of link beams, resulting in an increase in ductility.

4.3.2. Quantitative investigation of effective parameters in the behavior of box link beams with corrugated webs

Important seismic responses such as plastic rotational capacity, energy dissipation (relative to X2L1.2 specimen), elastic stiffness (relative to X2L1.2 specimen), and over-strength factor for box link beams with corrugated web are presented in Appendix A, which are further investigated in the following.

4.3.2.1. Plastic rotational capacity of box link beams with corrugated webs. Since shear force in short link beams is a displacement-controlled component, the plastic rotational capacity of link beams is the most important parameter for evaluating their performance. From the data

presented in Table A1 of Appendix A, it can be concluded that in the link beams with corrugated web, in addition to the compactness ratio of the web, the wavelength and the angle of the wave also affect the rotational capacity of the link beams. The method of changing the rotational capacity (without considering fracture in modeling) by changing the compactness ratio of the web, the number of waves throughout the link beam, and the angle of the wave are shown in Fig. 20. From Fig. 20a, it can be found that at the wave angle of 30°, most specimens are unable to achieve the target rotational capacity. Still, for bigger values of the wave angle (Fig. 20b), by decreasing the compactness ratio of the web and increasing the number of waves throughout the link beam, the rotational capacity of the link beam rises considerably. Based on Fig. 20c, it can be observed that in general, by decreasing the compactness ratio of the web and increasing the angle of the wave, the rotational capacity of the link beam increases, and the rate of this increase, increases with six waves in the length of the link beam (Fig. 20d). According to Fig. 20e, by increasing the angle of the wave and the number of waves throughout the link beam, the rotational capacity of the link beam increases and the rate of this increase is higher for the smaller compactness ratios of the web (Fig. 20f).

Note that the performance of shear link beams is acceptable if the plastic rotational capacity in these link beams is more than 0.08 rad. Consequently, determining geometric parameters of the corrugated web for the shear link beams is important for their behavior to be acceptable. Shahmohammadi et al. [30], to establish a relationship for rotational capacity in steel coupling beams with corrugated web, used the slenderness ratio of the corrugated web, which contains all the geometric properties of a corrugated plate. For design purposes and in the absence

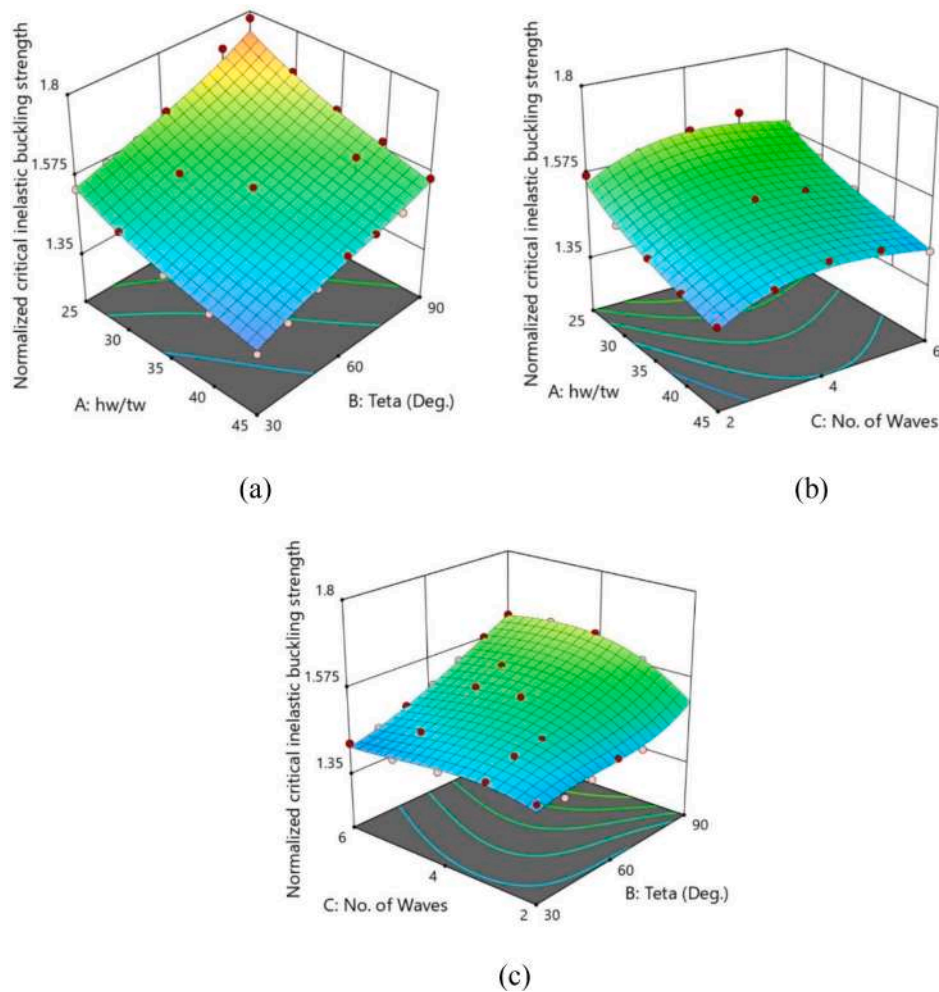


Fig. 17. Changes in the amount of inelastic shear capacity by changing: (a) the angle of the wave and the compactness ratio of the web, (b) the number of waves and the compactness ratio of the web, and (c) the wave angle and the number of waves.

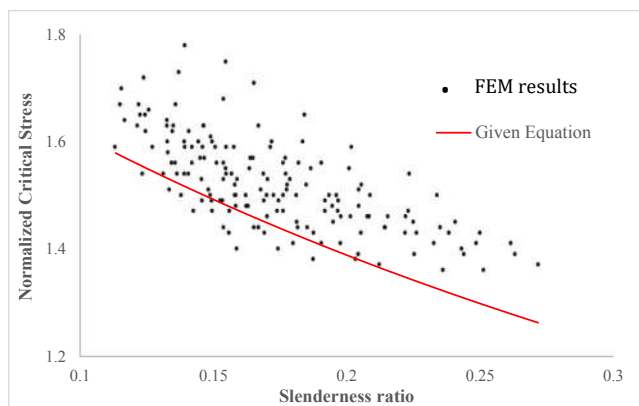


Fig. 18. Comparison between critical inelastic shear buckling stress versus slenderness ratio of the corrugated plate for Eq. (16) and modeling results.

of experimental data, In order for the plastic rotational capacity of box link beams with corrugated webs to be acceptable, the maximum allowable slenderness ratios for wave angles of 30°, 40°, 50°, 60°, 70°, 80°, and 90° were suggested 0.16, 0.17, 0.18, 0.19, 0.20, 0.21, and 0.23, respectively.

4.3.2.2. Energy dissipation capacity in the link beams. The changing

trend of the cumulative plastic energy dissipation in the box link beams till the target rotation (0.08 rad) compared to the energy dissipation in the X2L1.2 specimen, by changing the compactness ratio of the web and the number of waves throughout the link beam and the wave angle, is shown in Fig. 21. According to Fig. 21a, at a wave angle of 40°, the reduction of the compactness ratio of the web, regardless of the number of waves throughout the link beam, increases the energy dissipation. Still, at the wave angle of 70° and taking into account six waves throughout the link beam, the effect of the web compactness ratio on the energy dissipation of the specimen decreases (Fig. 21b). Increasing the number of waves from 2 to 4 throughout the link beams, at first, leads to a significant increase in energy dissipation. Still, with the further increase in the number of waves, the energy dissipation remains almost constant. The effect of the compactness ratio of the web and the angle of the wave on the energy dissipation of the link beams is shown in Fig. 21c and Fig. 21d. According to Fig. 21c, considering two waves throughout the link beam, the energy dissipation of the link beam increases by reducing the web compactness ratio and increasing the angle of the wave, but by increasing the number of waves throughout the link beams to 6 (Fig. 21d), increasing the wave angle first leads to an increase and then a decrease in the amount of energy dissipation. The way the energy dissipation changes with the changes in the number of waves throughout the link beams and the wave angle are also shown in Fig. 21e. According to Fig. 21e, increasing the number of waves from 2 to 4 increases the energy dissipation, but with the further increase in the number of waves, the energy dissipation remains constant. Also, increasing the angle of the

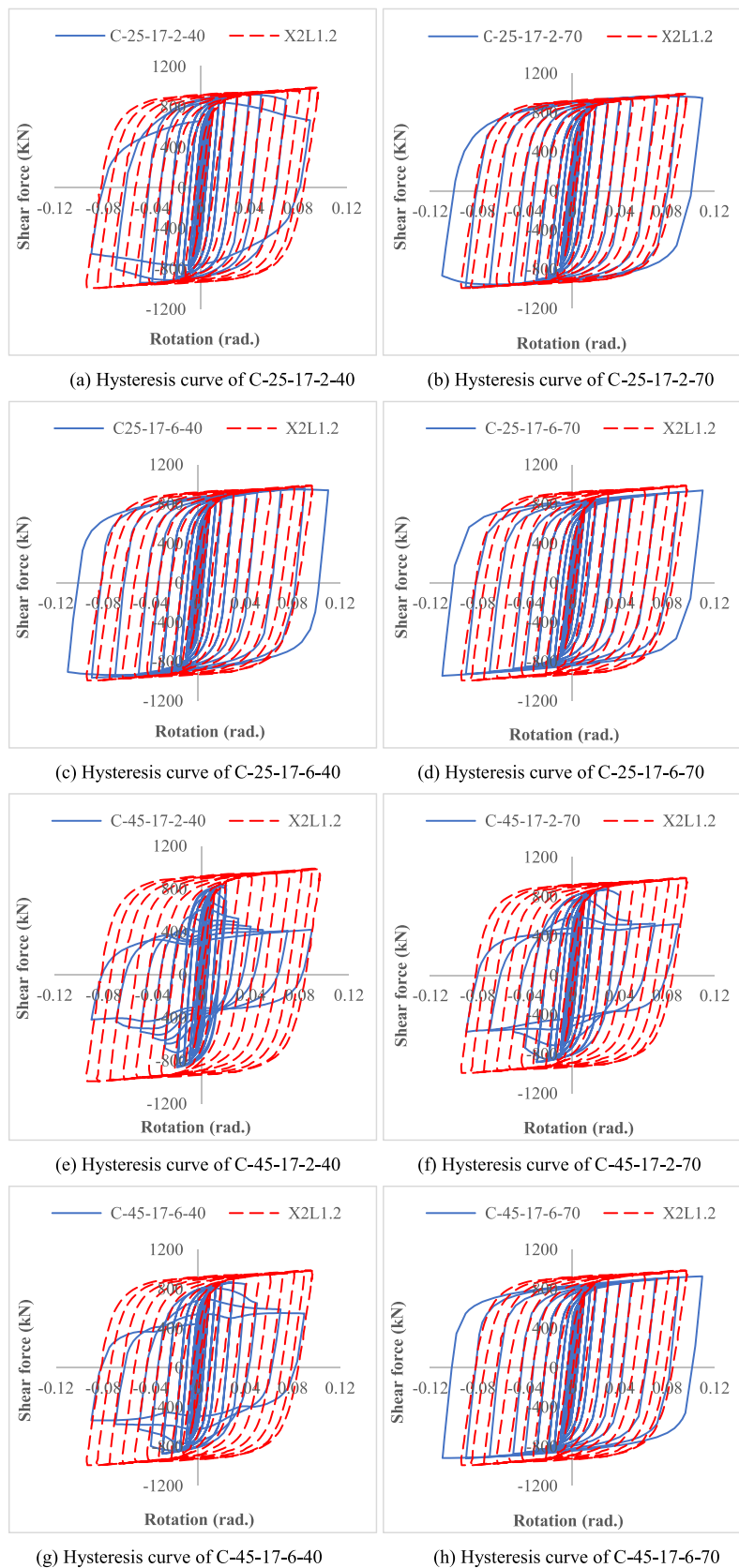


Fig. 19. Hysteresis curves of modeled specimens.

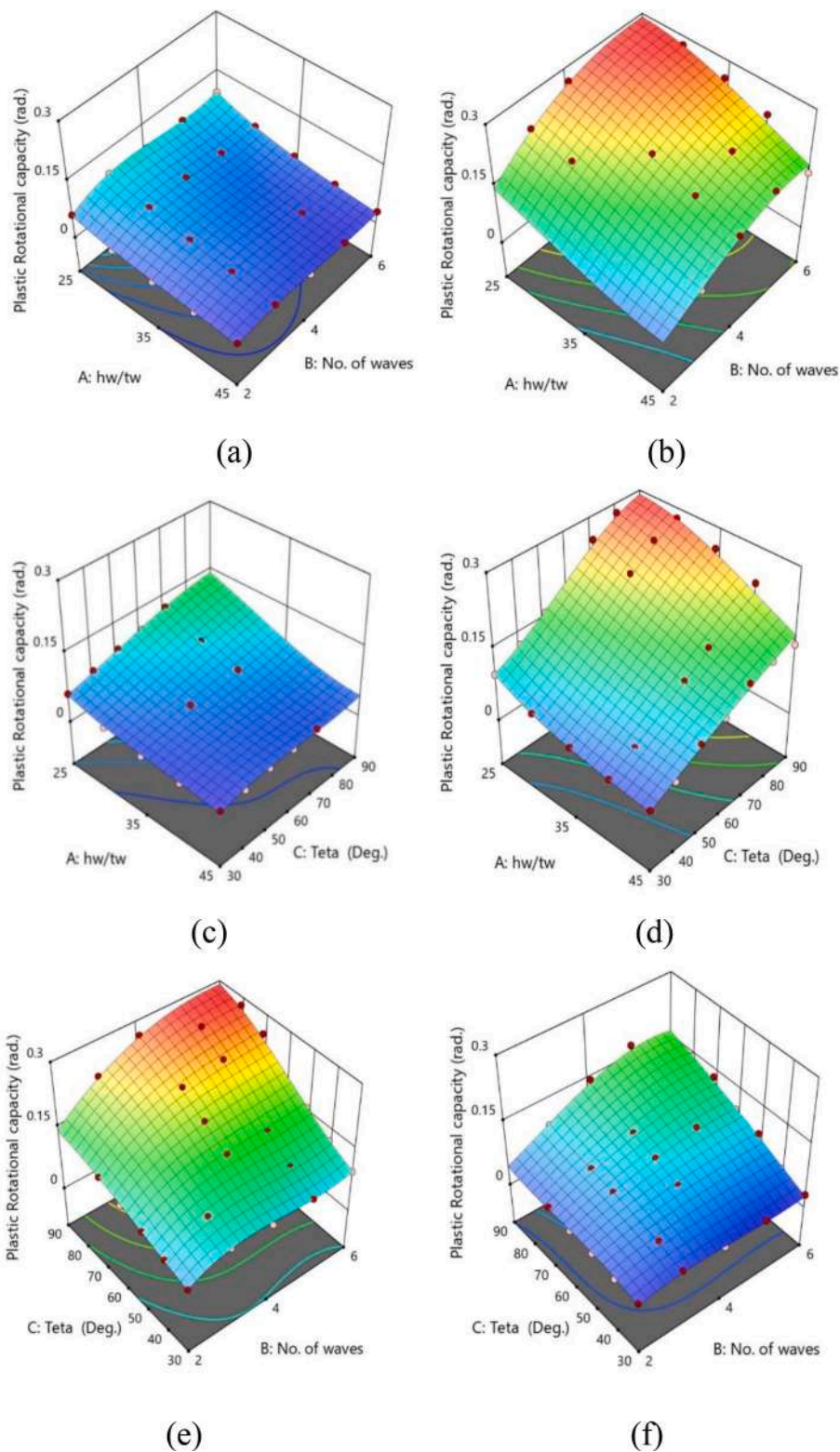


Fig. 20. Change trend in the rotational capacity of the link beams with: (a) wave angle of 30°, (b) wave angle of 90°, (c) two waves throughout the link beam, (d) six waves throughout the link beam, (e) web compactness ratio of 25, and (f) web compactness ratio of 45.

wave up to 70° increases the energy dissipation. With a further increase in the angle of the wave, the energy dissipation shows some reduction. In general, according to the presented Figures, the effect of the web compactness ratio on the energy dissipation of link beams with the corrugated web is greater than the effect of two parameters of the angle of the wave and the number of waves throughout the link beams; Also, as

mentioned above, increasing the angle of the wave does not necessarily increase the energy dissipation of the specimens; This can be attributed to the reduction of the plastic strain values of the diagonal sub-panels, by increasing the angle of the wave (less contribution of diagonal sub-panels in energy dissipation).

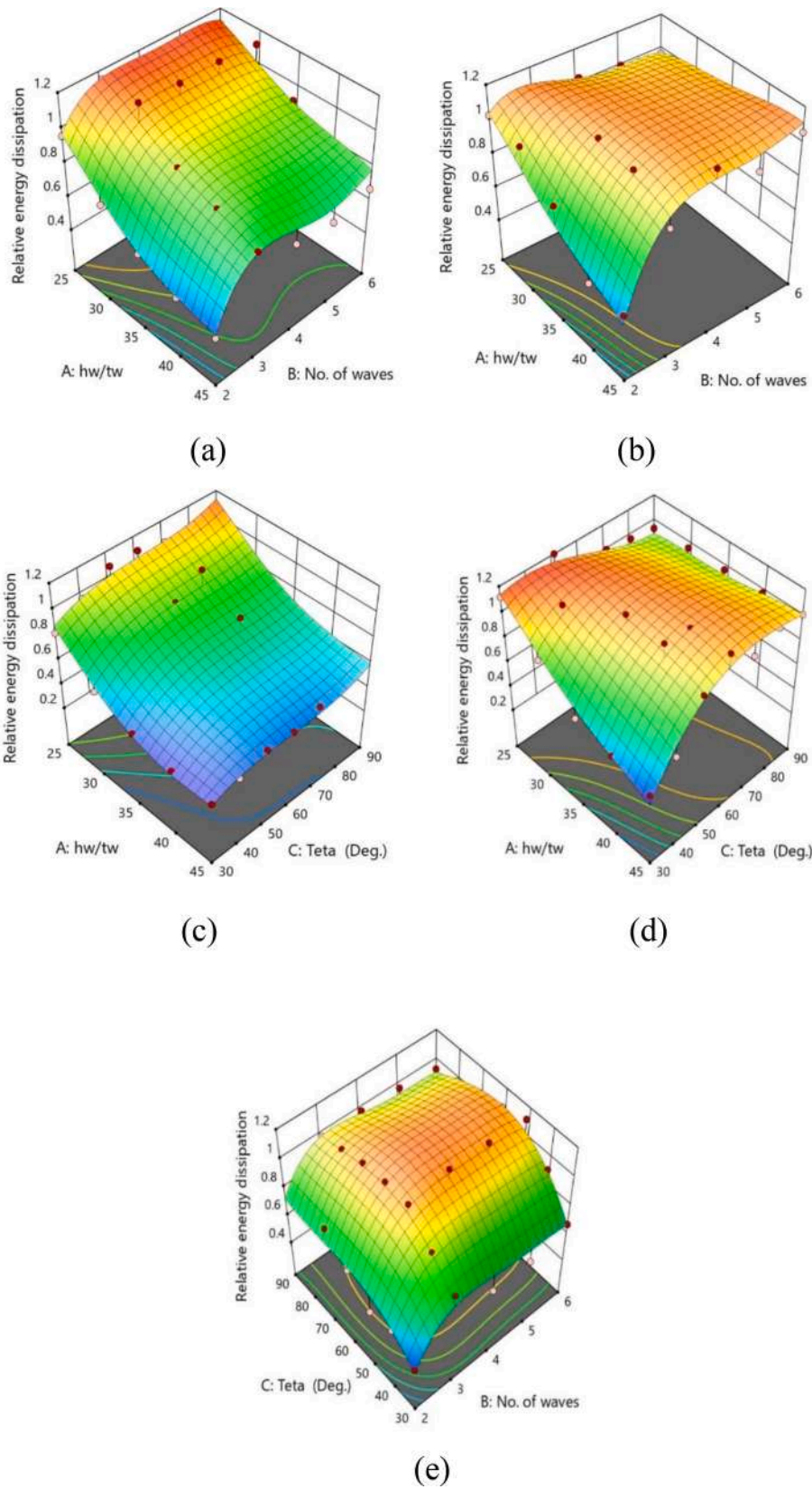


Fig. 21. Change of energy dissipation in the web of link beams with: (a) wave angle of 40°, (b) wave angle of 70°, (c) two waves throughout the link beam, (d) six waves throughout the link beam, and (e) web compactness ratio of 35.

4.3.2.3. *Elastic stiffness in the link beams with corrugated web.* From the data presented in Table A1 of Appendix A, it can be understood that the compactness ratio of the web and the number of waves throughout the link beams have an insignificant effect on the elastic stiffness of the box link beams, but increasing the wave angle reduces the flexural stiffness due to the increase of accordion effect and the decrease of shear stiffness in the web due to decrease of the web shear modulus. The changing trend of the elastic stiffness of modeled specimens compared to the X2L1.2 sample by changing different geometric parameters of the web is shown in Fig. 22.

4.3.2.4. *Over-strength factor in the link beams with corrugated web.* Based on the data presented in Table A1 of Appendix A, it can be found that the over-strength factor in the box link beams with trapezoidal corrugated webs in the modeled specimens is on average 1.45, and the value of the over-strength factor changes up to 30% by changing the geometric parameters in the corrugated web. The changing trend of the over-strength factor with the geometric parameters of the corrugated web is similar to the inelastic shear capacity of the link beams. Its value increases by decreasing the web's compactness ratio and increasing the wave's angle. Still, by increasing the number of waves throughout the link beams, its value rises first and then decreases.

5. Conclusion

Most of the research on using corrugated plates as the web of beams considered the web as a forced controlled element under gravity loads, and less attention has been paid to using the corrugated plates as a structural fuse undergoing inelastic excursions in cyclic loading. This study used trapezoidal corrugated plates as an alternative to flat webs in the box link beams with intermediate stiffeners. This makes the box link beam cheaper by reducing the amount of welding needed in the construction process and lowering the possibility of web fracture in the vicinity of the stiffener connection to the web of the link beam due to ultra-low cycle fatigue. Using corrugated webs in the box link beams increases the out-of-plane stiffness of the web plate and the buckling capacity in the box link beams without intermediate stiffeners. The most important geometric parameters affecting the behavior of trapezoidal corrugated web are the web compactness ratio, the wavelength, and the angle of the wave. In order to create a ductile and suitable behavior in the web of box link beams, in this study, the maximum compactness ratio of the web is considered to be 45. The values of wave angle and wave number throughout the link beams are also considered between 30° and 90° and 2 to 6, respectively. In order to investigate the effect of the mentioned geometric parameters, in this study, 170 box link beam

specimens were investigated by changing the geometrical characteristics. The results of this study are as follows:

- 1) Using Eigenvalue analysis in Abaqus software, it was found that the use of first-order interactive equation ($n = 1$) and global buckling coefficient ($\beta = 1.3$) provide the best results to determine critical elastic buckling stress; Also, the slenderness ratio decreased by decreasing the compactness ratio of the web plate. However, the changing trend in the slenderness ratio of the web plate was not certain by changing the wave angle and the number of waves in the link beam length and depends on the other geometric characteristics of the corrugated web.
- 2) By investigating the behavior of the specimens under monotonic loading, it was found that the critical inelastic buckling stress in the link beam specimens increased by decreasing the compactness ratio of the web plate and increasing the angle of the wave; However, the number of waves in the link beam length did not show a certain trend with the critical inelastic buckling stress. A lower band for the critical inelastic buckling stress of corrugated web plates can be estimated with using the relationship provided by Sause and Braxtan [15], assuming the values $u = 0.52$ and $n = 1$.
- 3) The plastic rotational capacity in the link beams with the trapezoidal corrugated web is generally subject to the compactness ratio of the web plate, the number of waves throughout the link beam, and the angle of the wave. Reduction of web compactness ratio and increasing the number of waves throughout the link beam and the wave angle increase the plastic rotational capacity of the link beams. The slenderness ratio of the corrugated plate can be used to determine the plastic rotational capacity of the link beams. The maximum allowable slenderness ratios to achieve target plastic rotation for wave angles of 30°, 40°, 50°, 60°, 70°, 80°, and 90° were 0.16, 0.17, 0.18, 0.19, 0.20, 0.21, and 0.23, respectively.
- 4) Cumulative energy dissipation in link beams under cyclic loading (up to 0.08 rad.) is an important parameter in evaluating the link beams' cyclic performance. Reduction of web compactness ratio increases energy dissipation in the link beams; In most cases, by increasing the number of waves throughout the link beam from 2 to 4, the amount of energy dissipation increases, but with the further increase in the number of waves throughout the link beam, the amount of energy dissipation remains almost constant; Also, mostly by increasing the angle of the waves from 30 to 70, the energy dissipation in the link beams shows an increase, but with the further increase of this parameter, the amount of plastic strain decreases in the diagonal panels. Thus the energy dissipation decreases in the link beams. In general, the compactness ratio of the web, the number of waves

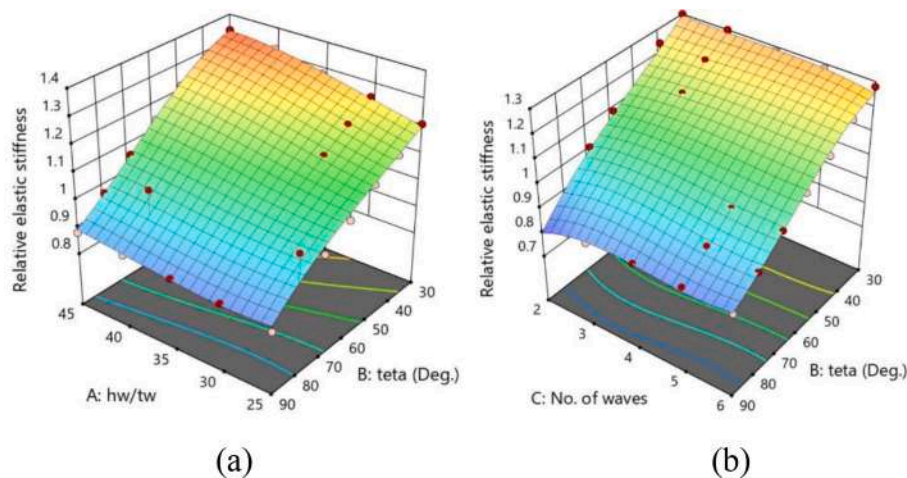


Fig. 22. Changes in the elastic stiffness of the link beams by changing the geometric parameters of the corrugated web (a) 4 waves throughout the link beams (b) the web compactness ratio equal to 35.

Table A1
Important responses in box link beams with corrugated web and flange compactness ratio of 17.

Name	Slenderness ratio	Normalized critical inelastic buckling strength by yield stress	Buckling mode	Plastic rotational capacity	Relative energy dissipation	Relative elastic stiffness	Over-strength factor
C-25-17-2-30	0.201	1.55	G	0.062	0.82	1.23	1.46
C-25-17-2-40	0.185	1.52	I	0.079	0.96	1.17	1.48
C-25-17-2-50	0.176	1.56	I	0.094	1.08	1.1	1.5
C-25-17-2-60	0.177	1.57	I	0.106	1.08	1.03	1.49
C-25-17-2-70	0.182	1.56	L	0.125	1.03	0.95	1.48
C-25-17-3-30	0.177	1.54	G	0.095	1.15	1.22	1.49
C-25-17-3-40	0.164	1.57	G	0.12	1.15	1.16	1.49
C-25-17-3-50	0.155	1.59	I	0.138	1.12	1.1	1.53
C-25-17-3-60	0.15	1.6	I	0.147	1.09	1.04	1.53
C-25-17-3-70	0.149	1.61	L	0.184	1.05	0.97	1.52
C-25-17-3-80	0.155	1.75	L	0.186	1.11	0.9	1.53
C-25-17-3-90	0.165	1.71	L	0.219	0.95	0.82	1.56
C-25-17-4-30	0.155	1.54	G	0.088	1.13	1.21	1.48
C-25-17-4-40	0.145	1.57	I	0.122	1.14	1.15	1.48
C-25-17-4-50	0.139	1.59	I	0.159	1.11	1.1	1.52
C-25-17-4-60	0.135	1.63	I	0.191	1.07	1.03	1.51
C-25-17-4-70	0.133	1.64	I	0.227	1.03	0.97	1.51
C-25-17-4-80	0.137	1.73	I	0.242	1.09	1.04	1.51
C-25-17-4-90	0.139	1.78	L	0.265	0.96	0.83	1.51
C-25-17-5-30	0.159	1.53	G	0.09	1.12	1.2	1.47
C-25-17-5-40	0.134	1.56	G	0.12	1.13	1.15	1.52
C-25-17-5-50	0.122	1.63	I	0.158	1.2	1.23	1.62
C-25-17-5-60	0.124	1.65	I	0.195	1.04	1.04	1.48
C-25-17-5-70	0.123	1.65	I	0.241	1	0.96	1.47
C-25-17-5-80	0.122	1.67	I	0.277	0.97	0.89	1.47
C-25-17-5-90	0.124	1.72	L	0.276	0.94	0.83	1.48
C-25-17-6-30	0.17	1.53	G	0.097	1.13	1.2	1.48
C-25-17-6-40	0.141	1.54	G	0.126	1.11	1.14	1.48
C-25-17-6-50	0.123	1.54	G	0.161	1.06	1.08	1.48
C-25-17-6-60	0.113	1.59	I	0.19	1.12	1.15	1.48
C-25-17-6-70	0.117	1.64	I	0.252	0.97	0.95	1.48
C-25-17-6-80	0.115	1.67	I	0.28	0.94	0.88	1.43
C-25-17-6-90	0.115	1.70	I	0.282	0.91	0.81	1.47
C-30-17-2-30	0.222	1.46	G	0.038	0.57	1.27	1.46
C-30-17-2-40	0.205	1.48	I	0.052	0.71	1.21	1.4
C-30-17-2-50	0.196	1.50	I	0.064	0.79	1.14	1.44
C-30-17-2-60	0.197	1.49	L	0.075	0.87	1.06	1.46
C-30-17-2-70	0.205	1.51	L	0.093	1	0.98	1.48
C-30-17-3-30	0.193	1.50	G	0.073	0.94	1.26	1.45
C-30-17-3-40	0.179	1.53	G	0.091	1.15	1.2	1.49
C-30-17-3-50	0.169	1.54	I	0.104	1.14	1.14	1.49
C-30-17-3-60	0.164	1.55	I	0.122	1.1	1.07	1.51
C-30-17-3-70	0.164	1.57	L	0.17	1.07	1	1.51
C-30-17-3-80	0.171	1.59	L	0.181	1.02	0.93	1.52
C-30-17-3-90	0.184	1.65	L	0.204	0.96	0.84	1.54
C-30-17-4-30	0.169	1.49	G	0.075	0.94	1.25	1.44
C-30-17-4-40	0.158	1.50	I	0.088	1.13	1.2	1.47
C-30-17-4-50	0.151	1.56	I	0.126	1.13	1.14	1.51
C-30-17-4-60	0.147	1.57	I	0.158	1.09	1.07	1.5
C-30-17-4-70	0.144	1.60	I	0.166	1.05	1	1.49
C-30-17-4-80	0.146	1.63	I	0.225	1.01	0.92	1.49
C-30-17-4-90	0.154	1.68	L	0.233	0.97	0.85	1.5
C-30-17-5-30	0.174	1.47	G	0.065	0.84	1.25	1.41
C-30-17-5-40	0.146	1.49	G	0.097	1.13	1.19	1.45
C-30-17-5-50	0.139	1.54	I	0.131	1.11	1.13	1.5
C-30-17-5-60	0.136	1.56	I	0.162	1.07	1.06	1.49
C-30-17-5-70	0.133	1.60	I	0.2	1.03	0.99	1.47
C-30-17-5-80	0.133	1.63	I	0.223	0.99	0.92	1.46
C-30-17-5-90	0.136	1.67	L	0.265	0.96	0.84	1.47
C-30-17-6-30	0.223	1.47	G	0.065	0.84	1.24	1.42
C-30-17-6-40	0.153	1.49	G	0.095	1.11	1.18	1.46
C-30-17-6-50	0.133	1.51	G	0.128	1.09	1.12	1.47
C-30-17-6-60	0.131	1.54	I	0.174	1.04	1.05	1.45
C-30-17-6-70	0.127	1.59	I	0.223	1	0.99	1.43
C-30-17-6-80	0.125	1.62	I	0.262	0.96	0.93	1.44
C-30-17-6-90	0.126	1.66	I	0.279	0.93	0.89	1.46
C-35-17-2-30	0.241	1.45	I	0.028	0.46	1.3	1.36
C-35-17-2-40	0.222	1.43	I	0.041	0.58	1.24	1.36
C-35-17-2-50	0.215	1.44	I	0.066	0.54	1.06	1.35
C-35-17-2-60	0.216	1.46	L	0.054	0.68	1.09	1.42
C-35-17-2-70	0.225	1.45	L	0.075	0.82	1.01	1.43
C-35-17-3-30	0.208	1.46	I	0.057	0.79	1.3	1.42
C-35-17-3-40	0.192	1.49	I	0.072	0.93	1.24	1.46

(continued on next page)

Table A1 (continued)

Name	Slenderness ratio	Normalized critical inelastic buckling strength by yield stress	Buckling mode	Plastic rotational capacity	Relative energy dissipation	Relative elastic stiffness	Over-strength factor
C-35-17-3-50	0.181	1.50	I	0.083	1.1	1.17	1.46
C-35-17-3-60	0.176	1.50	I	0.097	1.1	1.1	1.47
C-35-17-3-70	0.178	1.52	L	0.12	1.08	1.02	1.48
C-35-17-3-80	0.187	1.55	L	0.128	1.03	0.94	1.49
C-35-17-3-90	0.202	1.59	L	0.128	0.98	0.85	1.49
C-35-17-4-30	0.182	1.44	I	0.04	0.6	1.28	1.4
C-35-17-4-40	0.17	1.46	I	0.07	0.9	1.23	1.44
C-35-17-4-50	0.162	1.50	I	0.102	1.14	1.17	1.46
C-35-17-4-60	0.157	1.54	I	0.135	1.11	1.1	1.49
C-35-17-4-70	0.155	1.55	I	0.14	1.07	1.02	1.48
C-35-17-4-80	0.151	1.59	I	0.185	1.03	0.94	1.48
C-35-17-4-90	0.167	1.63	L	0.213	0.98	0.86	1.49
C-35-17-5-30	0.188	1.43	G	0.041	0.6	1.28	1.37
C-35-17-5-40	0.156	1.47	G	0.073	0.92	1.22	1.41
C-35-17-5-50	0.149	1.49	I	0.106	1.13	1.16	1.45
C-35-17-5-60	0.146	1.53	I	0.142	1.09	1.09	1.47
C-35-17-5-70	0.142	1.56	I	0.175	1.04	1.01	1.47
C-35-17-5-80	0.142	1.59	I	0.186	1.01	0.94	1.47
C-35-17-5-90	0.146	1.63	L	0.235	0.97	0.86	1.46
C-35-17-6-30	0.205	1.43	G	0.047	0.67	1.28	1.36
C-35-17-6-40	0.165	1.44	G	0.074	0.91	1.22	1.41
C-35-17-6-50	0.143	1.47	I	0.104	1.11	1.15	1.44
C-35-17-6-60	0.138	1.50	I	0.144	1.06	1.08	1.43
C-35-17-6-70	0.136	1.54	I	0.182	1.02	1.01	1.43
C-35-17-6-80	0.133	1.58	I	0.207	0.98	0.93	1.44
C-35-17-6-90	0.135	1.62	I	0.256	0.94	0.85	1.42
C-40-17-2-30	0.263	1.39	I	0.025	0.4	1.33	1.32
C-40-17-2-40	0.243	1.40	I	0.033	0.49	1.27	1.34
C-40-17-2-50	0.235	1.44	I	0.036	0.51	1.2	1.35
C-40-17-2-60	0.239	1.43	L	0.04	0.55	1.12	1.38
C-40-17-2-70	0.25	1.43	L	0.043	0.54	1.03	1.38
C-40-17-3-30	0.226	1.43	G	0.046	0.68	1.32	1.39
C-40-17-3-40	0.209	1.46	I	0.063	0.85	1.26	1.43
C-40-17-3-50	0.197	1.47	I	0.07	0.89	1.2	1.44
C-40-17-3-60	0.192	1.47	I	0.08	1.04	1.13	1.44
C-40-17-3-70	0.195	1.48	L	0.096	1.06	1.04	1.46
C-40-17-3-80	0.206	1.52	L	0.105	1.05	0.95	1.48
C-40-17-3-90	0.224	1.54	L	0.105	0.99	0.86	1.49
C-40-17-4-30	0.198	1.41	I	0.033	0.53	1.32	1.36
C-40-17-4-40	0.185	1.44	I	0.053	0.75	1.26	1.41
C-40-17-4-50	0.176	1.47	I	0.086	1.11	1.19	1.45
C-40-17-4-60	0.17	1.50	I	0.123	1.12	1.12	1.48
C-40-17-4-70	0.168	1.51	I	0.118	1.08	1.04	1.48
C-40-17-4-80	0.172	1.60	I	0.136	1.12	1.05	1.55
C-40-17-4-90	0.184	1.60	L	0.176	1	0.87	1.49
C-40-17-5-30	0.204	1.39	G	0.036	0.54	1.31	1.35
C-40-17-5-40	0.169	1.43	I	0.063	0.82	1.25	1.41
C-40-17-5-50	0.162	1.48	I	0.096	1.12	1.19	1.45
C-40-17-5-60	0.158	1.48	I	0.129	1.1	1.11	1.46
C-40-17-5-70	0.154	1.53	I	0.16	1.06	1.04	1.46
C-40-17-5-80	0.154	1.56	I	0.166	1.02	0.95	1.45
C-40-17-5-90	0.158	1.59	L	0.21	0.98	0.87	1.46
C-40-17-6-30	0.226	1.39	G	0.036	0.55	1.31	1.33
C-40-17-6-40	0.18	1.41	G	0.062	0.81	1.25	1.39
C-40-17-6-50	0.156	1.43	I	0.087	1.09	1.18	1.42
C-40-17-6-60	0.15	1.47	I	0.126	1.09	1.11	1.44
C-40-17-6-70	0.148	1.51	I	0.16	1.04	1.03	1.44
C-40-17-6-80	0.139	1.60	I	0.168	1.07	1.04	1.5
C-40-17-6-90	0.146	1.59	I	0.227	0.96	0.86	1.45
C-45-17-2-30	0.272	1.37	I	0.025	0.39	1.36	1.3
C-45-17-2-40	0.251	1.36	I	0.027	0.43	1.3	1.31
C-45-17-2-50	0.244	1.39	I	0.034	0.5	1.22	1.35
C-45-17-2-60	0.249	1.41	L	0.036	0.49	1.14	1.36
C-45-17-2-70	0.262	1.41	L	0.043	0.54	1.05	1.38
C-45-17-3-30	0.233	1.41	G	0.036	0.58	1.35	1.36
C-45-17-3-40	0.214	1.44	G	0.054	0.77	1.29	1.41
C-45-17-3-50	0.195	1.45	I	0.054	0.82	1.37	1.5
C-45-17-3-60	0.198	1.46	I	0.069	0.86	1.15	1.43
C-45-17-3-70	0.201	1.46	L	0.077	0.9	1.06	1.43
C-45-17-3-80	0.209	1.50	L	0.082	1.07	1.09	1.53
C-45-17-3-90	0.234	1.50	L	0.09	0.95	0.87	1.46
C-45-17-4-30	0.203	1.38	I	0.027	0.45	1.34	1.34
C-45-17-4-40	0.191	1.41	I	0.043	0.65	1.28	1.38
C-45-17-4-50	0.181	1.45	I	0.075	0.95	1.22	1.43
C-45-17-4-60	0.175	1.49	I	0.093	1.11	1.14	1.45

(continued on next page)

Table A1 (continued)

Name	Slenderness ratio	Normalized critical inelastic buckling strength by yield stress	Buckling mode	Plastic rotational capacity	Relative energy dissipation	Relative elastic stiffness	Over-strength factor
C-45-17-4-70	0.173	1.50	I	0.107	1.1	1.06	1.46
C-45-17-4-80	0.178	1.51	L	0.121	1.05	0.97	1.47
C-45-17-4-90	0.191	1.56	L	0.146	1	0.88	1.48
C-45-17-5-30	0.212	1.37	G	0.028	0.47	1.34	1.33
C-45-17-5-40	0.174	1.40	I	0.042	0.62	1.28	1.36
C-45-17-5-50	0.167	1.44	I	0.076	0.95	1.21	1.41
C-45-17-5-60	0.163	1.48	I	0.111	1.12	1.14	1.44
C-45-17-5-70	0.158	1.50	I	0.11	0.96	0.94	1.26
C-45-17-5-80	0.158	1.52	I	0.143	1.04	0.97	1.45
C-45-17-5-90	0.165	1.57	L	0.178	1.01	0.88	1.45
C-45-17-6-30	0.236	1.36	G	0.03	0.49	1.05	1.3
C-45-17-6-40	0.187	1.38	G	0.047	0.67	1.27	1.36
C-45-17-6-50	0.159	1.40	I	0.085	1.04	1.2	1.39
C-45-17-6-60	0.154	1.44	I	0.1	1.1	1.13	1.42
C-45-17-6-70	0.153	1.49	I	0.135	1.06	1.05	1.43
C-45-17-6-80	0.149	1.50	I	0.145	1.01	0.96	1.43
C-45-17-6-90	0.141	1.62	I	0.146	1.12	1	1.58

throughout the link beam, and the wave angle had the greatest impact on the specimens' energy dissipation, respectively. If the geometric parameters of the link beams with the corrugated web are properly selected, energy dissipation in these link beams can be up to 20% more than that of in the link beams with flat web and intermediate stiffeners.

- 5) The elastic stiffness of the box link beams with trapezoidal corrugated webs is only subject to the angle of the wave but independent of the compactness ratio of the web and the number of waves throughout the link beam. By increasing the wave angle, the elastic stiffness of the specimens decreases linearly.
- 6) The amount of over-strength factor in the box link beams with trapezoidal corrugated web increases by decreasing the compactness ratio of the web plate and increasing the angle of the wave, but by increasing the number of waves throughout the link beam, the amount of over-strength factor rises first and then shows a decrease. The average value of the over-strength factor measured in the box link beams with the corrugated web was 1.45, which is approximately equal to the over-strength factor suggested for typical box link beams.
- 7) Considering the increase in steel consumption, the weight of the link beams, and the reduction in elastic stiffness and energy dissipation in wave angles greater than 70°, the maximum wave angle in the web of box link beams is suggested to be 70°. Also, due to small rotational capacity and energy dissipation in specimens with a 30° wave angle, the minimum wave angle is recommended to be equal to 40°.

Declaration of Competing Interest

The authors declare that they have no known competing financial interests or personal relationships that could have appeared to influence the work reported in this paper.

Appendix A

Important specifications such as slenderness ratio of the web plate, critical inelastic buckling stress, plastic rotational capacity, energy dissipation of the specimens compared to X2L1.2 specimen, elastic stiffness of specimens compared to X2L1.2 specimen, elastic buckling mode, and over-strength factor for the box link beams with corrugated web and flange compactness ratio of 17 are presented in Table A1. It should be noted that the elastic buckling mode of the corrugated web is marked by the letters "G" meaning global buckling, "L" meaning local buckling, and "I" meaning interactive buckling.

References

- [1] Popov EP, Kasai K, Engelhardt MD. Advances in design of eccentrically braced frames. *Earthq Spectra* 1987;3(1):43–55.
- [2] Aisc. Specification for Structural Steel Buildings. Chicago, USA: American Institute of Steel Construction; 2016.
- [3] Bruneau M, Uang CM, Sabelli R. Ductile design of steel structures. McGraw-Hill Education; 2011.
- [4] Berman JW, Bruneau M. Approaches for the seismic retrofit of braced steel bridge piers and proof-of-concept testing of an eccentrically braced frame with tubular link. Multidisciplinary Center for Earthquake Engineering Research 2005.
- [5] Berman JW, Bruneau M. Further development of tubular eccentrically braced frame links for the seismic retrofit of braced steel truss bridge piers. 2006 Mar 27.
- [6] Kasai K, Popov EP. Cyclic web buckling control for shear link beams. *J Struct Eng* 1986;112(3):505–23.
- [7] Lian M, Guan B, Cheng Q, Zhang H, Su M. Experimental and numerical study of seismic performance of high-strength steel fabricated framed-tube structures with replaceable shear links. *Structures* 2020;28:2714–32.
- [8] Elgaaly M, Seshadri A, Hamilton RW. Bending strength of steel beams with corrugated webs. *J Struct Eng* 1997;123(6):772–82.
- [9] Elgaaly M, Hamilton RW, Seshadri A. Shear strength of beams with corrugated webs. *J Struct Eng* 1996;122(4):390–8.
- [10] Driver RG, Abbas HH, Sause R. Shear behavior of corrugated web bridge girders. *J Struct Eng* 2006;132(2):195–203.
- [11] Abbas HH, Sause R, Driver RG. Shear strength and stability of high performance steel corrugated web girders. *Proceedings, Structural Stability Research Council 2002*;361–87.
- [12] Sayed-Ahmed EY. Behaviour of steel and (or) composite girders with corrugated steel webs. *Can J Civ Eng* 2001;28(4):656–72.
- [13] Yi J, Gil H, Youm K, Lee H. Interactive shear buckling behavior of trapezoidally corrugated steel webs. *Eng Struct* 2008;30(6):1659–66.
- [14] El Metwally A, Loov RE. Corrugated steel webs for prestressed concrete girders. *Mater Struct* 2003;36(2):127–34.
- [15] Sause R, Braxtan TN. Shear strength of trapezoidal corrugated steel webs. *J Constr Steel Res* 2011;67(2):223–36.
- [16] Nie JG, Zhu L, Tao MX, Tang L. Shear strength of trapezoidal corrugated steel webs. *J Constr Steel Res* 2013;85:105–15.
- [17] Riahi F, Behraves A, Fard MY, Armaghani A. Shear buckling analysis of steel flat and corrugated web I-girders. *KSCE J Civ Eng* 2018;22(12):5058–73.
- [18] Elkawas AA, Hassanein MF, El-Boghdadi MH. Numerical investigation on the nonlinear shear behaviour of high-strength steel tapered corrugated web bridge girders. *Eng Struct* 2017;134:358–75.
- [19] Leblouba M, Junaid MT, Barakat S, Altoubat S, Maalej M. Shear buckling and stress distribution in trapezoidal web corrugated steel beams. *Thin-Walled Struct* 2017; 113:13–26.
- [20] Leblouba M, Barakat S, Al-Saadon Z. Shear behavior of corrugated web panels and sensitivity analysis. *J Constr Steel Res* 2018;151:94–107.
- [21] EN 1993-1-5. Eurocode 3: Design of Steel Structures, Part 1–5: Plated Structural Elements. 2005.
- [22] Lho SH, Lee CH, Oh JT, Ju YK, Kim SD. Flexural capacity of plate girders with very slender corrugated webs. *International Journal of Steel Structures* 2014;14(4): 731–44.
- [23] Abbas HH. Analysis and design of corrugated web I-girders for bridges using high performance steel. Lehigh University 2003.
- [24] Kövesdi B, Jáger B, Dunai L. Stress distribution in the flanges of girders with corrugated webs. *J Constr Steel Res* 2012;79:204–15.
- [25] Cafolla J. Corrugated webs and lateral restraints in plate girders for bridges. University of Warwick; 1995. Doctoral dissertation.
- [26] Li GQ, Jiang J, Zhu Q. Local buckling of compression flanges of H-beams with corrugated webs. *J Constr Steel Res* 2015;112:69–79.

- [27] Sherman D, Fisher J. Beams with corrugated webs. 1st International Specialty Conference on Cold-Formed Steel Structures. 1971.
- [28] Elamary AS, Alharthi Y, Abdalla O, Alqurashi M, Sharaky IA. Failure mechanism of hybrid steel beams with trapezoidal corrugated-web non-welded inclined folds. *Materials* 2021;14(6):1424:1–18.
- [29] Ibrahim SA, El-Dakhkhni WW, Elgaaly M. Behavior of bridge girders with corrugated webs under monotonic and cyclic loading. *Eng Struct* 2006;28(14):1941–55.
- [30] Shahmohammadi A, Mirghaderi R, Hajsadeghi M, Khanmohammadi M. Application of corrugated plates as the web of steel coupling beams. *J Constr Steel Res* 2013;85:178–90.
- [31] Hajsadeghi M, Zirakian T, Keyhani A, Naderi R, Shahmohammadi A. Energy dissipation characteristics of steel coupling beams with corrugated webs. *J Constr Steel Res* 2014;101:124–32.
- [32] Emami F, Mofid M, Vafai A. Experimental study on cyclic behavior of trapezoidally corrugated steel shear walls. *Eng Struct* 2013;48:750–62.
- [33] Aisc. Seismic Provisions for Structural Steel Buildings. Chicago, USA: American Institute of Steel Construction; 2002.
- [34] Chaboche JL. Time-independent constitutive theories for cyclic plasticity. *Int J Plast* 1986;2(2):149–88.
- [35] Behbahani DP, Fanaie N. Elimination of intermediate stiffeners in box link beam using low yield point steel. *Journal of Constructional Steel Research*. 2022. 188: 107014.
- [36] AC 154. Acceptance criteria for cyclic racking shear tests for metal-sheathed shear walls with steel framing. ICC Evaluation Service, INC; 2008.
- [37] Lindner J, Huang B. Beulwerte für trapezförmig profilierte Bleche unter Schubbeanspruchung. *Der Stahlbau* 1995;12:370–4.
- [38] Easley JT, McFarland DE. Buckling of light-gage corrugated metal shear diaphragms. *J Struct Div* 1969;95(7):1497–516.
- [39] Moon J, Yi J, Choi BH, Lee HE. Shear strength and design of trapezoidally corrugated steel webs. *J Constr Steel Res* 2009;65(5):1198–205.
- [40] Timoshenko SP, Gere JM. *Theory of Elastic Stability*, Mineola. 2009.
- [41] Hassanein MF, Kharoob OF. Behavior of bridge girders with corrugated webs :(I) Real boundary condition at the juncture of the web and flanges. *Eng Struct* 2013; 57:554–64.
- [42] Richards PW, Uang CM. Testing protocol for short links in eccentrically braced frames. *J Struct Eng* 2006;132(8):1183–91.